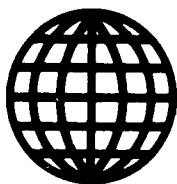


JPRS-JST-90-048

29 OCTOBER 1990



**FOREIGN  
BROADCAST  
INFORMATION  
SERVICE**

# ***JPRS Report***

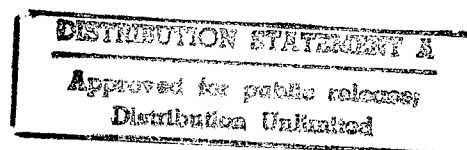
# **Science & Technology**

***Japan***

27TH AIRCRAFT SYMPOSIUM

DTIC QUALITY INSPECTED 3

REPRODUCED BY  
U.S. DEPARTMENT OF COMMERCE  
NATIONAL TECHNICAL INFORMATION SERVICE  
SPRINGFIELD, VA. 22161



19980203 321

JPRS-JST-90-048  
29 OCTOBER 1990

## SCIENCE & TECHNOLOGY JAPAN

### 27TH AIRCRAFT SYMPOSIUM

906C3832 Tokyo HIKOKI SHINPOJIUMU in Japanese 18-20 Oct 89 pp 1-124

[Selected papers presented at the 27th Aircraft Symposium held 18-20 Oct 89 in Kyushu]

#### CONTENTS

Optical Sensor Technology Applications [Hiroshi Anegawa, Yasushi Wakabayashi, et al.].....	1
In-Space Laser Communication Technology [Hiroshi Arikawa, Yasumasa Hisada, et al.].....	7
Optical Technology Applied to On-Board Electronic Equipment [Yasushi Sakurai].....	14
Optical Data Bus Technology Applications for Spacecraft [Hiroshi Anegawa, Horishi Arikawa].....	20
Fly-By-Light Element Technology Development [Mitsuyoshi Mayanagi].....	27
Application of Optical Communication Parts to Optical Data Bus [Takeshi Sugawa, Yasunori Murakami].....	36
R&D of Passive Optical Gyro [Kazuo Hotate, Minoru Higashiguchi].....	43
Sawtooth Wave Generation Circuit on Closed Loop Fiber Gyro [Akihiro Kurokawa, Kenichi Kajiwara, et al.].....	53
In-Flight Imaging System [Takashi Kijima, Hiroshi Asano].....	60

Optical Applied Equipment in Aeronautical Field [Daigen Kuroshima, Shunichi Nishimura].....	65
STOL Aircraft HUD Radar Guidance Landing Test [Kenji Yazawa, Kazuya Masui].....	70
Estimated Flight-Path Angle Display [Kazuya Masui, Kenji Yazawa].....	77

## **Optical Sensor Technology Applications**

906C3832A Tokyo HIKOKI SHINPOJIUMU in Japanese 18-20 Oct 89 pp 64-67

[Article by Hiroshi Anegawa, Yasushi Wakabayashi, Isao Kono, Mitsushige Oda, and Taichi Nakamura, National Space Development Agency of Japan]

### **[Text] 1. Introduction**

As measuring sensors carried by spacecraft, optical sensors such as earth sensors, sun sensors, fixed star sensors, and ring laser gyros have to date been utilized in navigation guidance control. In addition, however, hopes are placed on applying optical sensor technology to new fields such as spaceship rendezvous and docking and space robots for activities in the space infrastructure age of the future. In this paper, proximity optical sensors for docking spaceships are described, with emphasis on rendezvous radars currently being trial manufactured by NASDA. Further, concepts on and prospects for visual sensors for space robots are described.

### **2. Optical Sensor Technology for Rendezvous and Docking**

The spaceship rendezvous and docking technology is a fundamental technology indispensable for future space activities. Unlike the Apollo and Gemini projects, changes in requirements from manual to automatic rendezvous and docking and from impact to soft docking are accelerating the practical application of optical sensor technology as highly accurate sensors.

#### **(1) Laser Radar (Rendezvous Radar)**

Rendezvous radars are used after the approach stage (within several kilometers from the target) of the rendezvous sequence, based on relative navigation. Unlike conventional RF radars, rendezvous radars use a laser radar system for the highly accurate short distance measurements necessary for automatic rendezvous. Rendezvous radars can measure relative distance, relative speed, direction angles (line of sight (LOS) angle), relative attitude, etc., with respect to the target spacecraft.

As shown in Figure 1, a target spacecraft has a laser reflector, called "corner cube reflector" (CCR), based on a cooperative passive system that

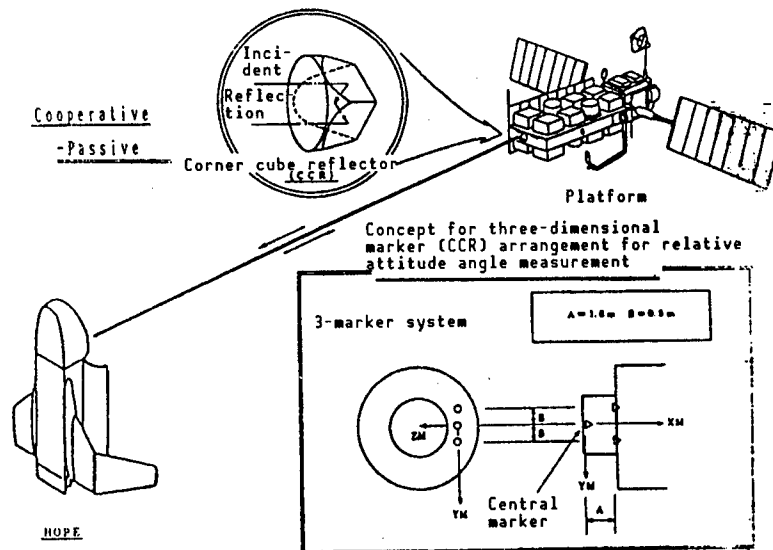


Figure 1. Concepts on Rendezvous Radar Measurements

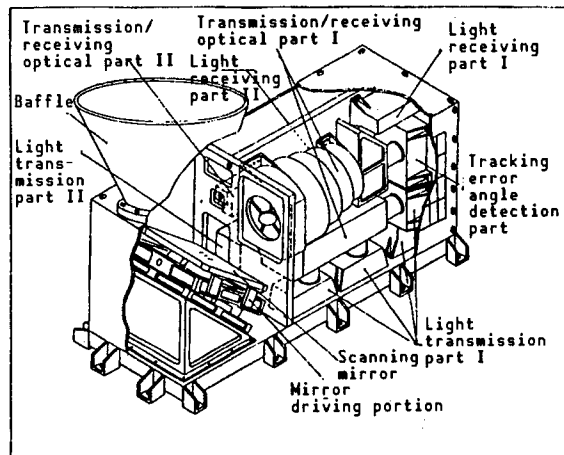


Figure 2. Concepts on Rendezvous Radar (head portion)

makes it possible to construct the simplest entire system. Using light reflecting from the laser reflector, relative distance, relative speed, etc., are measured.

Figure 2 shows the concept for a rendezvous radar. It is a tracking type radar and carries out measurements while catching and tracking the target spacecraft. The functions can be classified roughly into catching, tracking, distance measurement (including speed and LOS angles), and relative attitude angle measurements.

Catching the target spacecraft is carried out by raster scanning laser beams (beam spread angle:  $0.05^\circ$ ) within a range of about  $3^\circ \times 3^\circ$ , using a two-axial gimbal mirror based on rough LOS angle information provided by the navigation system. Tracking the target spacecraft is carried out by detecting light reflected from the CCR, using a quadrant detector (QD) and by driving/

controlling the gimbal mirror so that the error signal becomes zero. Further, by detecting the drive angle when the error signal becomes zero, LOS angles are measured. Amplitude of the laser beam is modulated with tone frequency, and phase differences in the transmission/receiving signals are measured; thus, distance is measured. Further, to precisely measure distance based on phase differences equivalent to values obtained by multiplying wavelength by integers, and to improve measuring accuracy within a short distance range, several tone frequencies are used. For measuring relative speed, differences in measured distance data and direct measurements using a subcarrier Doppler system are properly used according to distance. Further, the two-dimensional pattern of a CCR located on the target spacecraft is detected by a charged-coupled device (CCD) within a short distance (less than 200 m), and attitude angles are calculated based on that two-dimensional pattern. Such a relative attitude measuring system is being studied.

Further, since 1987, tests using a prototype have been conducted with the aim of obtaining basic data concerning the following items that are thought to be particularly critical:

- Scanning/tracking driving system:
  - Bearing (flexural pivot)
  - Angle encoder
- Transmission/receiving optical part
- Light receiving part preamplifier

Acquisition of primary data necessary for future research has already been completed, except for evaluation (being currently conducted) of the transmission/receiving optical part environmental characteristics.

## (2) Proximity Optical Sensor

Proximity optical sensors are used for measuring short distances—within tens of meters, much shorter than the range of use by rendezvous radars—for controls prepared for final docking. The required type of proximity sensors must be studied on the basis of requirements arising from berthing and docking contact conditions. Proximity sensors must also be studied as a system for allotment of work between proximity sensors and rendezvous radars, etc. NASDA has started such studies this year. A variety of systems can be considered for obtaining distance and attitude information in proximity regions. An example of such a system is shown in Figure 3, and an outline is described below. An example of an optical sensor system is also shown in Figure 4.

### 1) Marker Sensor System

The marker sensor system consists of several three-dimensional or two-dimensional markers located on the target spacecraft which are detected by CCD sensors, etc., installed on the chaser spacecraft. From the positional relation between the markers, navigation information (relative position) is obtained. One marker sensor system uses light emitting diodes (LED) and CCRs

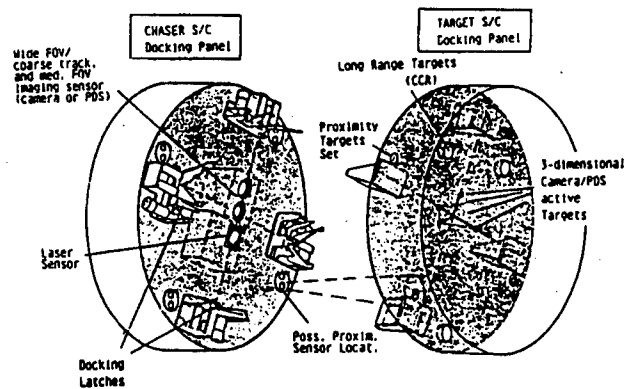


Figure 3. Example of Proximity Optical Sensor System

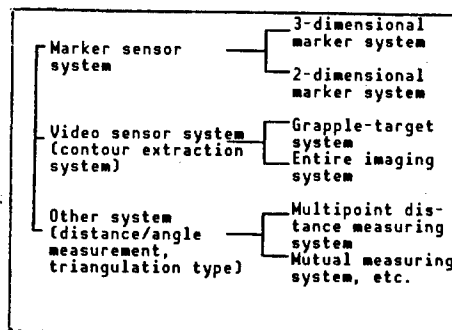


Figure 4. Example of Optical Sensor for Rendezvous/Docking

as markers. Another system uses CCDs and position sensitive devices (PSD) as detectors. The algorithm of the marker sensor system is not complicated, unlike the video sensor system discussed below, thus making it possible to carry out high-speed calculations. The marker sensor system, therefore, can be said to be suitable for real-time processing. The three-dimensional marker system employs the same process as the rendezvous radar relative attitude measuring system. In the two-dimensional marker system, markers are located in the inertial main axial direction on the target surface. Then, using the projection geometry knowledge, the direction cosine of each axis is obtained, based on coordinates of the focal point on the screen and distance between the visual point and the screen; the relative attitude is then determined.

## 2) Video Sensor System

Specific patterns (grapple target, etc.) drawn on the target spacecraft, or the entire target spacecraft, is imaged by camera. Navigation information is obtained by on-board image processing, such as extraction of contours and template matching. The use of the video sensor system results in an increase in the volume of calculations compared with the marker sensor system. This system, however, can flexibly comply with a wide range of requirements, and is a future system on which many hopes are placed.

An internationally standard figure called "grapple target" located in the vicinity of the grapple fixture on the target spacecraft is imaged by camera. Contour lines and turning points are extracted by processing such as matching and dichotomizing into two values. On the basis of the coordinates (distance and gradient) of the feature points, navigation information is obtained (Figure 5). This is the grapple target system.

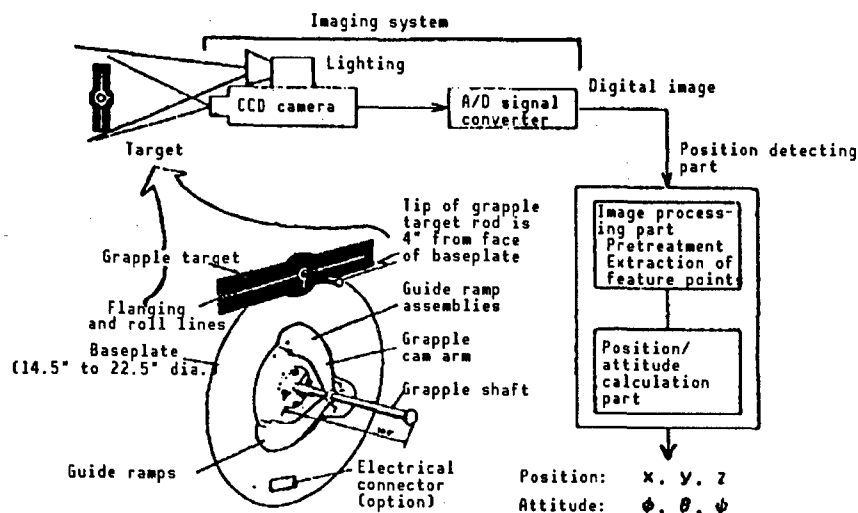


Figure 5. Measuring Concept on Grapple Target System

The grapple target system has many applications immediately before docking and has internationally common features by using grapple targets. For an entire imaging system, the entire target spacecraft is imaged by camera, and contour lines are extracted by dichotomizing into two values, etc. Template matching is then carried out, using spacecraft shape data, and navigation information is obtained. Unlike other systems, the grapple target system bases its use on a slightly long distance range (10 m or more). In particular, restrictions on hardware such as markers are not imposed on target spacecraft except for the use of target shape data.

### 3) Other Systems

#### Multipoint Distance Measuring System:

A multipoint measuring system uses laser radars to detain relative positions and relative attitudes by measuring the distance to several markers (CCR) and azimuth (LOS angles). The relative attitude angle measuring accuracy depends on distance measuring accuracy. If the distance measuring accuracy is assumed to be 5 cm, the relative attitude angle measuring accuracy is not satisfactory, that is,  $4^\circ$ . This system, however, does not require the use of other hardware to measure relative attitudes and can measure all relative attitudes using only one laser radar.



### Mutual Measuring System (Figure 6):

An optical sensor (laser radar or CCD camera) possessing LOS angle measuring functions is also installed on the target spacecraft. Thus, on the basis of the LOS angle observed from the target spacecraft and that observed from the chaser, relative attitude and distance are obtained. In this case, it is necessary to install a laser radar on the target spacecraft and to transmit LOS angle information to the chaser side. The mutual measuring system is thus subject to large restrictions, but it does not require complicated operation processing. Further, high measuring accuracy (a superior feature of laser measurements) can be utilized to a maximum extent, and the highest measuring accuracy can be obtained for relative attitude angles.

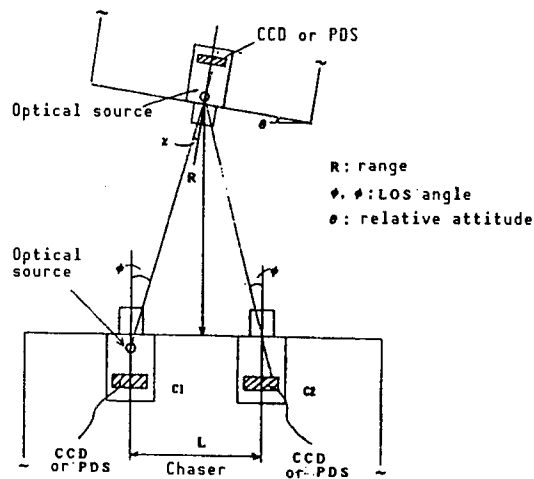


Figure 6. Measuring Concept of Mutual Measuring System

### 3. Application to Space Robot Visual Sensor

Many information-recognition technologies are necessary if space robots are to carry out their work. With regard to visual sensors of such technologies, basic technologies such as laser radars for rendezvous docking, range finders, and video sensors will be utilized. These technologies are expected to be further developed in the future (Figure 7 shows one application concept).

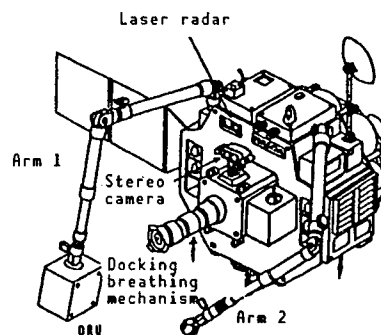


Figure 7. Application to Space Robot

## In-Space Laser Communication Technology

906C3832B Tokyo HIKOKI SHINPOJIUMU in Japanese 18-20 Oct 89 pp 68-71

[Article by Hiroshi Arikawa, Yasumasa Hisada, and Hiroshi Anegawa, National Space Development Agency of Japan; Koichi Shiratama, NEC Corp., and Koichi Komatsu, Toshiba Corp.]

### [Text] 1. Introduction

Laser communications in space makes it possible not only to transmit data in large quantities, but also to prevent mutual interferences. Laser communications also make it possible to get large antenna gains and to reduce the system size and weight. Further, laser communications are not affected by the atmosphere, clouds, rain, etc., and many hopes are placed on this as the next-generation space communications. This paper reports an outline of space laser communications being implemented at the NASDA Tsukuba Space Center.

### 2. Inter-Satellite Laser Communication System

Concepts for an inter-satellite laser communication system are shown in Figure 1. The system is assumed to be for communications between geostationary orbital satellites, such as the data relay tracking satellite (DRTS) and low to intermediate altitude satellites, the so-called Geostationary Earth Orbit-Low Earth Orbit (GEO-LED) communications. The GEO-LED technology, if it is developed as a catching and tracking technology (a critical technology), appears to be applicable to GEO-GEO communications.

Basic concepts for a laser communication system structure are shown in Figure 2.

It is important to select an appropriate wavelength in developing space optical devices. Two wavelengths, the 0.85  $\mu\text{m}$  and 1.3  $\mu\text{m}$  bands, were selected, based on the use of semiconductor laser diodes (LD) carried by spacecraft, maturity of technology, and prospective application. Of these two wavelengths, the 0.85  $\mu\text{m}$  band (for which a two-dimensional CCD is available for catching and tracking) was selected for catching and tracking. To achieve laser communications between satellites, the technical problems such as aberration, Doppler deflection, effect of background noise, and enhancement of laser

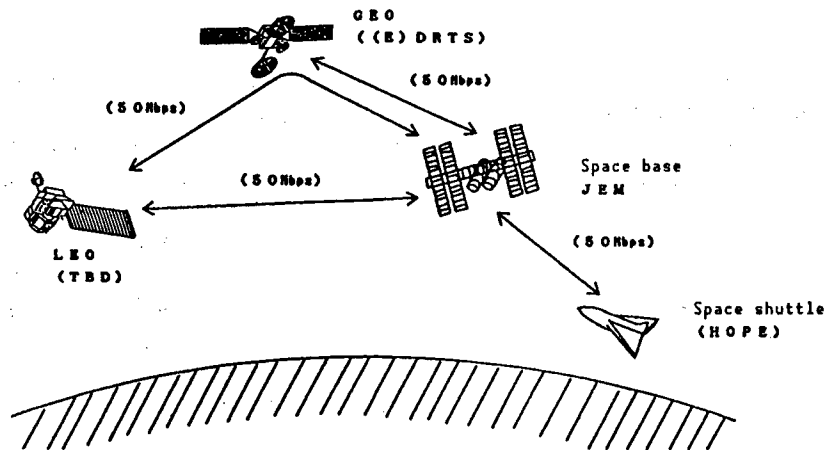


Figure 1. Concept for Laser Communications in Space

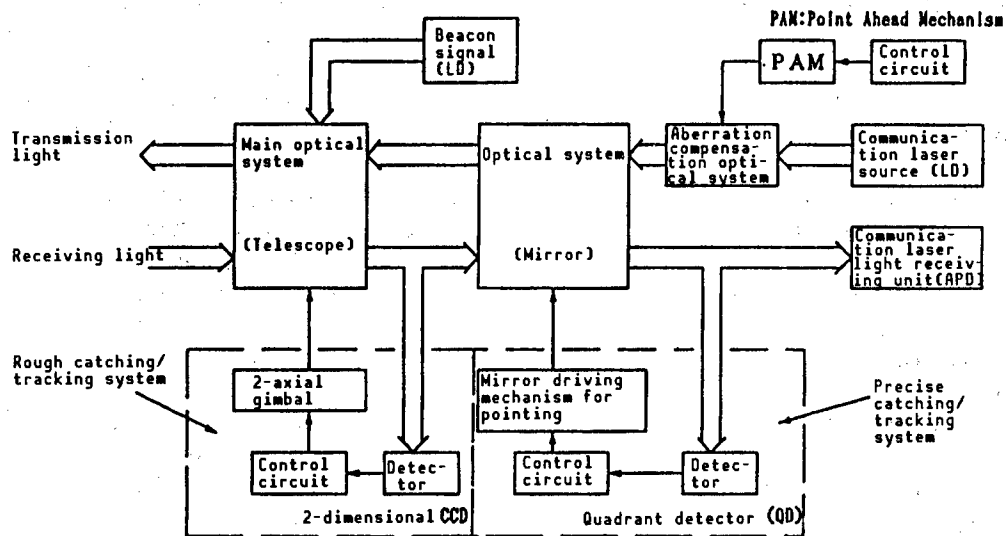


Figure 2. Basic Concepts on Laser Communication System Structure

output must be studied. To establish circuits, it is necessary to sharply reduce laser beams and, therefore, to accurately carry out beam pointing. The establishment of a highly accurate catching/tracking technology, therefore, will become one of the most important development tasks.

### 3. Study and Trial Manufacture of Catching/Tracking System

The catching/tracking system consists of the following two systems:

- Rough catching/tracking system, in which directional control of beams is carried out extending over a wide range ( $360^\circ$ ) and at low speed (3 deg/s).
- Precise catching/tracking system, in which directional control of beams is carried out with high accuracy (within  $\pm 1 \mu\text{rad}$ ) and at high speed (50 Hz or more).

The precise catching/tracking system is a technology indispensable for and peculiar to the system that links satellites with a narrow beam of about  $10\ \mu\text{rad}$ . The actuator of the precise catching/tracking system, therefore, underwent trial manufacture and tests between 1987 and 1988; selected as candidates were 1) a piezoelectric actuator system, and 2) a moving coil system. Further, trial manufacture and tests are being conducted (between 1988 and 1989) to evaluate the entire catching/tracking system including the above actuators. These two types of actuators and the results of trial manufacture and test on the catching/tracking system are described below.

#### (1) Trial Manufacture and Tests Based on Piezoelectric Actuator System

In the piezoelectric actuator system, a laminated piezoelectric actuator is installed on the angle displacement mechanism as a precise catching/tracking system mirror-driving mechanism. The angle displacement mechanism converts the longitudinal displacement of a laminated piezoelectric actuator (expanding and contracting from applied voltage) to the angle of the mirror's deviation. A combination of angle displacement mechanism with a laminated piezoelectric actuator makes it possible to achieve a friction-free mirror driving system, ensuring high resolution, high speed, low power consumption, and low noise.

Further, quadrant detectors (QD) are used for detecting errors in received beam angles. QD output signals undergo signal processing, fed back to the control circuit, and are used to control the mirror driving mechanism so that received beams come to the center of the QD. To detect received beams, the modulating signal detecting system is used. This system detects modulating signals (modulation factor: about 10 percent, about 20 kHz)—superimposed on beams—that are not likely to be affected by the direct-current optical level. Thus, measures are taken for background light. With respect to control characteristics, an accuracy of  $\pm 40\ \mu\text{rad}$  and a speed of 1 Hz were assumed as a change in the attitude of satellites due to thrusters, etc. It is intended that the target spacecraft is tracked within an accuracy of  $\pm 1\ \mu\text{rad}$ . In addition, PID control is used for the control circuit with consideration given to low harmonic attitude changes and the hysteresis of the mirror driving mechanism, etc. As the loop gain of the control system, 32 dB or larger (1 Hz) and 52 dB or larger (0.1 Hz), therefore, become necessary.

A mirror driving mechanism shown in Figure 3 was manufactured for experiments. A precise catching/tracking system was then formed and testing was conducted. As a result, the following mirror driving mechanism performance was obtained.

- Driving angle range: about 73 mrad, equivalent to  $\pm 3.65\ \text{mrad}$  in terms of an optical antenna (magnification: 20 times) incident beam angle
- Hysteresis: maximum 9 mrad
- Resolution:  $3\ \mu\text{rad}$  or less
- Resonant frequency: about 130 Hz

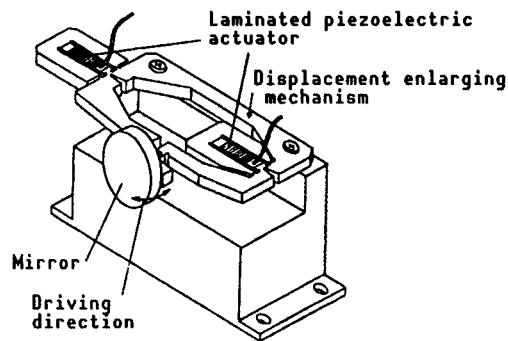


Figure 3. Piezoelectric Actuator System

The control characteristics of the precise catching/tracking system are given in Table 1. With respect to tracking accuracy, beams equivalent to  $\pm 40 \mu\text{rad}$  (fluctuation frequency: 1 Hz) incident on an optical antenna, were incident on the mirror used under testing conditions, and the tracking error angle in regard to such beams was measured. As a result, a tracking performance of about  $\pm 0.75 \mu\text{rad}$  was confirmed to be obtained under a change in the angle of incident beams ( $\pm 40 \mu\text{rad}$ ).

Table 1. Piezoelectric FPM Control Characteristics

Item	Characteristics		Remarks
	Target performance	Test results	
Drive angle range	$\geq \pm 0.017^\circ$ ( $\pm 300 \mu\text{rad}$ )	$\pm 0.21^\circ$ ( $\pm 3.65 \text{ mrad}$ )	Optical antenna incident beam angle
Tracking accuracy	$\pm 1 \mu\text{rad}$	$\pm 0.75 \mu\text{rad}$	Same as above
Frequency characteristics			
Open loop gain	$\geq 32 \text{ dB}$	36 dB	at 1 Hz
	$\geq 52 \text{ dB}$	56 dB	at 0.1 Hz
Phase margin	$\geq 30 \text{ deg}$	30 deg	

Conditions:

- Optical antenna incident beam angle fluctuation
- Optical antenna magnification

## (2) Trial Manufacture and Test Based on Moving Coil System

A moving coil is installed (as a actuator) on the mirror driving mechanism used for the precise catching/tracking system. Figure 4 illustrates the experimental actuator.

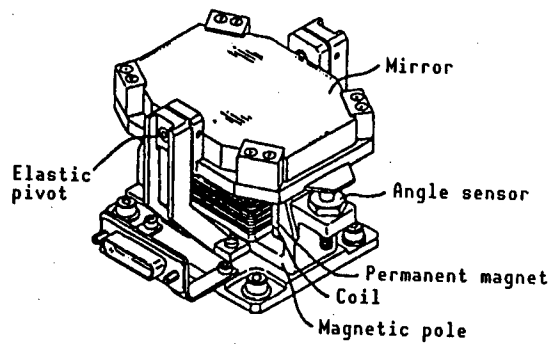


Figure 4. Moving Coil System

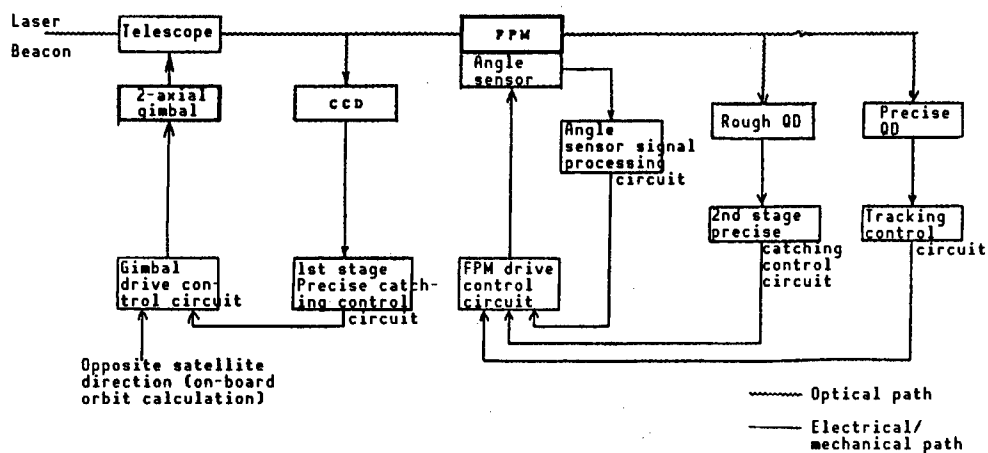


Figure 5. Catching/Tracking System Functional Block Diagram  
(Moving coil system FPM)

Figure 5 shows a functional block diagram on the catching/tracking system based on the moving coil system. Further, Table 2 presents the results of a study of the major component specifications.

A sequence leading from catching to tracking is described below.

1) Rough catching: Catching/tracking communication signals sent by the opposite satellite are introduced within the specified range of the rough catching sensor (CCD) by controlling two-axial gimbal pulse counts (program control).

2) Precise catching: After completion of rough catching, catching/tracking communication signals sent by the opposite satellite are introduced within the specified range of the precise catching sensor (QD).

(1) First-stage precise catching: The two-axial gimbal is closed-loop controlled, so that the catching sensor (CCD) signals become zero. In this case, the fine pointing mechanism (FPM) is maintained at the zero point by angle control (digital PID control).

Table 2. Specifications of Moving Coil System Catching/Tracking System

Element	Item	Design target value
Optical system	Diameter (mm)	100
	Magnification	60
2-axial gimbal (trial manufacture of only Az)	Drive range (deg)	X±22/AZ ±1800 Y±22/E <sub>l</sub> 0~115
	Drive speed (deg/s)	03/3.0
	Drive resolution (deg)	0.0036
FPM	Drive range (deg)	1.0
	Control bandwidth (Hz)	200~1000
CCD	Visual field (mrad)	6.97
	Resolution (μrad)	29
Rough QD	Visual field (mrad)	1.67
	Resolution (μrad)	17
Precise QD	Visual field (mrad)	69.4
	Resolution (μrad)	0.7

(2) Second-stage precise catching: If beams are caught within the visual field of the precise catching sensor (rough QD), the FPM is closed-loop controlled, so that the precise catching sensor output becomes zero. In this case, closed-loop control of the two-axial gimbal by CCD is continued (analog PID control).

(3) Tracking: After completion of catching, tracking signals are maintained within the specified range of the tracking sensor (precise QD), and the FPM is closed-loop controlled, so that the tracking sensor signals become zero. In this case, closed-loop control of the two-axial gimbal by CCD is continued (analog PID control).

This catching/tracking system is characterized by the lowering of requirements for the drive resolution with respect to the two-axial gimbal to a figure that may be achievable (that is, about 0.0035° as a result of system study). Also, to minimize directional errors in the first stage precise catching, the gap (dominant factor resulting in errors) between the two-axial gimbal bearing and housing and the control system dead band, directional error allotments have been set at 0.006° and 0.009°, respectively.

#### 4. Conclusion

Laser communication technologies in space were described, with emphasis on the catching/tracking technology that is thought to be particularly important, reporting the results of trial manufacture and tests. We intend to start trial manufacture on a full scale, while obtaining further necessary basic data.



## **Optical Technology Applied to On-Board Electronic Equipment**

906C3832C Tokyo HIKOKI SHINPOJIUMU in Japanese 18-20 Oct 89 pp 72-75

[Article by Yasushi Sakurai, Toshiba Corp.]

### **[Text] 1. Introduction**

Optical technology applied electronic equipment has made marked progress in recent years,<sup>1,2</sup> and is receiving much attention in electronic equipment carried by aircraft (hereinafter referred to as "on-board electronic equipment"). Thus, many items of applied optical technology equipment are being studied for practical use.<sup>3,4,5,6</sup>

This paper reviews the possible application of optical technology to on-board electronic equipment and presents prospects for the development of future equipment.

### **2. Specific Features of Light<sup>7,8,9,10,11</sup>**

#### **(1) Large Signal Transmission Capacity**

Extremely large signal transmission capacity is ensured by separating the wavelengths in a single transmission medium into many channels.

#### **(2) Ultrahigh Speed Propagation**

High frequency results in high time resolution. Light is not affected by capacitance, surface effects, etc., and it is possible to transmit signals at high speed.

#### **(3) Nonelectromagnetic Inductivity**

Optical signals are not affected by inductive or radioactive noise and have superior electromagnetic impulse (EMI) resistivity.

#### **(4) Coherent Light Having Highly Practical Applicability**

Coherent light from a laser is coherent, monochromatic, beam directable, and light condensable, and has large output, short pulse generation, etc.

### **3. Requirements for Future On-Board Electronic Equipment<sup>12,13,14,15,16</sup>**

#### **(1) Improvement of Storm and EMI Resistivity**

- Prevention of breakage due to lightning, malfunction, etc.
- Taking measures for aggravated EMI environment.

#### **(2) High-speed Data Processing**

- Real-time processing of large amount of data
- Real-time processing of AI algorithms

#### **(3) Highly Advanced Man-Machine Interface**

- Proper judgment in an extensive amount of information

#### **(4) Miniaturizing/Lightweight**

- Carrying many items of equipment in a limited space
- Reduction of weight for fuel saving

#### **(5) Highly Resistible to Disturbance and Detection Retardant (Military use)**

- Avoiding being detected by electronic measures
- Taking measures for electromagnetic disturbance

### **4. Application of Optical Technology to On-Board Electronic Equipment<sup>3,4,7,14,15</sup>**

To comply with a variety of requirements for on-board electronic equipment, optical technology applied aircraft electronic equipment that takes advantage of specific features of light is being developed in various fields. Table 1 presents optical technology applied on-board electronic equipment that already has been put into practical use or is being studied for practical use.

### **5. Prospects for Future On-Board Electronic Equipment**

The major items of optical technology applied on-board electronic equipment currently being studied for practical use are outlined below.

#### **5.1 Optical Computer<sup>8,9,13,16,17</sup>**

Research is being conducted on optical computers for processing a large amount of data and AI algorithms at high speed. That optical computers could greatly exceed the capacity limit of electronic computers has recently begun to be recognized. Two types of optical computers are being studied: Neumann type and non-Neumann type. The specific feature of each are given in Table 2.

Table 1. Optical Technology Applied to On-Board Electronic Equipment

Equipment field	Requirements for future on-board electronic equipment	Optical technology applied on-board electronic equipment
Sensors	Improvement of measuring accuracy Improvement of target-discriminating performance	Laser radar Optical spare
Data processing/transmission	High-speed/parallel processing Large-capacity data processing/accumulation Improvement of EMI and EMP resistivity	Optical computer Optical disk memory Optical data bus
Man/machine interface	Integration of data indication Improvement of observation performance	Helmet-mounted sight Holographic display
Communication	Noise resistance Secrecy (military use)	Laser communication Blue green laser
Navigation	Alignment time reduction Improvement of maintainability Strap down	Ring laser gyro (RLG) Fiber optical gyro (FOG)

Table 2. Specific Features of Optical Computer

Architecture	Operation system	Specific features
Time series system (Neumann type)	Electrooptics	<ul style="list-style-type: none"> <li>• Conventional computer architecture and software can be used</li> <li>• Concurrent use of electronic arithmetic part and optical arithmetic part</li> </ul>
Parallel system (non-Neumann type)	Parallel analog	<ul style="list-style-type: none"> <li>• Parallel processing of analog image data</li> <li>• High-speed parallel processing in extremely natural form</li> </ul>
	Parallel digital	<ul style="list-style-type: none"> <li>• Ultraparallelism of light and flexibility of digital operation</li> <li>• Parallel optical connection, thereby eliminating complicated wiring</li> </ul>
	Optical neuro	<ul style="list-style-type: none"> <li>• Ultradispersion and ultraparallel processing using neuro network</li> <li>• Intellectual data processing, capable of associative storage</li> </ul>

Time-series optical computers are manufactured by replacing conventional electronic computer parts with optical devices. It is expected that an operation capacity of  $10^2$  to  $10^3$  times that of current supercomputers can be obtained by improving switching and memory access speeds, using the high-speed characteristics of light.

The architecture of parallel optical computers is non-Neumann architecture. This eliminates von-Neumann bottlenecks (due to bus competition) and clock skews arising from propagation delay, etc. Parallel optical computers, therefore, can be expected to carry out operations at a capacity of  $10^6$  to  $10^9$  times that of supercomputers by using the ultraparallelism and an ultrawide band of light.

The parallel analog system uses optical operation filters and can achieve high-speed data processing that results in extremely high parallelism for specific purposes. This system, however, cannot be widely used for various purposes and, therefore, highly accurate data processing cannot be expected. Unlike the parallel analog system, the parallel digital system ensures accurate and flexible data processing and is receiving much attention as a general-purpose ultrahigh-speed computer. Optical neuro computers have an architecture that imitates the data processing mechanism of the living brain, and hopes are placed on its use for the AI system.

## 5.2 Holographic Display<sup>14,18,19</sup>

Two types of holograms are capable of displaying three-dimensional images: optical holograms and computer holograms. Optical holograms cannot be prepared without actual objects. Computer holograms eliminate this need for actual objects, requiring only sampled data be input into the computer. Computer holograms can be applied to various fields. As aircraft electronic equipment, computer holograms might be used as holographic displays that display the attitude of an aircraft's airframe and topography as three-dimensional images.

Computer holograms can display deep images. This system makes it possible to observe the side, etc., of displayed objects by changing the line-of-sight direction, thereby facilitating sensuous grasping of the condition of objects. It is possible, therefore, to properly recognize the attitude of an aircraft's own airframe and uneven topography and, thereby, to safely operate the aircraft during bad weather or low-altitude night-time flight. As a cockpit in which a holographic display is introduced to display attitudes, the one shown in Figure 1 [not reproduced] is being designed.

There are displays that display holographic images using animation, data processing system that processes a large quantity of data (necessary for three-dimensional images) on a real-time basis, etc. These are elements to be developed toward achievement of the system.

## 6. Conclusion

Many requirements for future aircraft electronic equipment may be achieved by applying optical technology. At present, some elements still need to be developed, such as optical materials and optical devices. Therefore, it will take more time to be able to apply optical materials, optical devices, etc., to the entire aircraft electronic equipment system. However, the application of optical materials, etc., to the entire system will make it possible to achieve light, small-size aircraft electronic equipment superior in EMI resistivity, and to achieve avionics that allow signal processing without conversion loss. Application of optical technology to aircraft electronic equipment, therefore, will further be promoted.

## References

1. "Trend of Optical Industry in 1988," Optical Industrial Technology Promotion Association, March 1989.
2. "Optical Technology Applied System Feasibility Study Report IX," Ibid., 1989.
3. Gamou, H., "Prospects for Ring Laser Gyro Technology," O PLUS E, No 10, 1982.
4. Takizawa, M., "Research on One-Way Moving Wave Ring Laser Gyro (I)," NATIONAL AEROSPACE LABORATORY RESEARCH REPORT, 1988.
5. "Report on Research and Investigation of Innovated Aircraft Technology Development Including Results," Japan Aerospace Industrial Society, No 912, 1985.
6. Ibid., No 6005, 1986.
7. Anegawa and Kawanishi, "Study of Concept on Space Optical Data Bus," TECHNICAL REPORT, COMMUNICATIONS ACADEMIC SOCIETY, Vol 87 No 16, SANE87-28, 1984.
8. Tai, et al., "Optical Neuro Computer," ELECTRONIC ACADEMIC SOCIETY JOURNAL, Vol 109 No 6, 1989.
9. Ishikawa, M., "Optical Computing," COMMUNICATIONS ACADEMIC SOCIETY JOURNAL, No 72 No 2, 1989.
10. Sakurai, et al., "Practical Laser Technology," Electronic Communications Academic Society, 1983.
11. Shimada, "Current Status and Prospects," COMMUNICATIONS ACADEMIC SOCIETY JOURNAL, Vol 72 No 2, February 1989.

12. "Report on Research and Investigation of Innovated Aircraft Technology Development Including Results," Japan Aerospace Industrial Society, No 814, 1984.
13. Yatagai, T., "Current Status of and Problems in Optical Computer Research," APPLIED PHYSICS, Vol 57 No 8, 1988.
14. "Military Use of Laser," Federation of Economic Organization, Defense Production Committee, 1986.
15. Fujisawa, A., "Recent Military Electronic Optical Technology," O PLUS E, No 7, 1984.
16. Ichioka and Yada, "Parallel Digital Optical Computer," Extra Issue Science, 1987.
17. Yatagai, T., "Parallel Digital Optical Operation Method," OPTOELECTRONICS, No 7, 1988.
18. Swihart, J.M., "Aeronautical Development for the 21st Century," 1987.
19. Tsujiuchi, "Optical Data Processing," Asakura bookstore, 1974.

## **Optical Data Bus Technology Applications for Spacecraft**

906C3832D Tokyo HIKOKI SHINPOJIUMU in Japanese 18-20 Oct 89 pp 76-79

[Article by Hiroshi Anegawa and Hiroshi Arikawa, National Space Development Agency]

### **[Text] 1. Introduction**

Space activities in the coming age of on-orbit infrastructure greatly differ from conventional concepts. To cope with such space activities, it is necessary to make rapid progress in both quality and quantity of the functions and performance of the data bus carried by future spacecraft. The optical data bus, which uses optical fibers for data transmission, is an optical data transmission system in optical computer. The optical data bus possesses superior characteristics, and hopes are placed on it being the next-generation data bus. This paper describes future research and development concepts and problems for optical data bus use in space.

### **2. Limit of Electric Data Bus and Features of Optical Data Bus**

Several tens of Mbps to several hundred Mbps data transmission capacity is estimated to be necessary for the data transmission system for future spacecraft such as platforms. A conventional electron data bus for use in satellites has the following data transmission limits.

(1) Data transmission speed: about 0.5 Mbps.

(2) Data transmission distance: about 30 m. Higher speed data transmission results in a shorter data transmission distance, that is 1 m.

(3) EMI on bus line: It is possible to increase the data transmission speed to about 10 Mbps by using coaxial cables, etc. It is necessary, however, to bypass thick, heavy shields and harnesses to counteract EMI. Thus, an electron data bus for satellites is limited for use in spacecraft. Further, it is not possible to transmit data at a transmission speed of several hundred Mbps.

In the case of an optical data bus, however, the wide band of optical signals allows communications to be carried out at high speed and in high volume.

The use of optical fibers eliminates problems such as deterioration of high frequency characteristics, damping, impedance mismatching, etc., arising from conductor skin effects (involved in high-speed communications as in the case of metal wires), flotation capacity, etc. In addition, optical fibers can minimize loss and waveform distortion. Optical fibers, therefore, allow data transmission over long distances and over longer interterminal distances, thus being suitable for use in future large spacecraft. Optical signals also are superior in EMI resistivity, and optical fibers are not electrical conductors. Thus, an optical data bus guarantees transmission signal quality and eliminates concern about current leakage, crosstalk, short circuit failures, and generation of sparks. It is not necessary to provide grounding. An optical data bus can also electronically separate components. Its nonsusceptibility to EMI greatly improves the packaging of the system. (Packaging with other lines or any equipment is possible and shielding is not necessary.) Thus, an optical data bus makes it possible to greatly reduce the weight and volume of the system. The effect of weight reduction differs according to spacecraft size, data transmission speed, etc. The larger the size of the spacecraft and the higher the data transmission speed, the more the effect of weight reduction increases in an exponential and functional manner. Further, data can be transmitted without multiplying wavelengths and bringing transmission lines into direct contact with each other. These are characteristics peculiar to "light," and light has many possibilities. Table 1 lists the features of optical data bus.

Table 1. Features of Optical Data Bus

- |     |   |
|-----|---|
| (1) | High speed/large capacity data transmission (wide band)   |
| (2) | Longer interterminal distance   |
| (3) | Strong resistivity to EMI   |
| (4) | —Improvement of channel integrity<br>—Improvement of packaging<br>—Design/test labor saving   |
| (5) | Electrical separation between components<br>—Elimination of effects of charges (no sparks/explosion)<br>—No short circuit failures, etc.  |
| (6) | Simplification of instrumentation (harness) system<br>—Return (ground) line: not necessary<br>—Optical fiber: small diameter and flexible |
| (7) | Small size and light weight   |
| (8) | Others (future potentiality)<br>• Multiplying wavelength is possible<br>• Compatibility of wire with wireless                             |

### 3. Current Status of and Problems With Optical Data Bus Technology

Japan's optical device technology ranks top in the world, and Japan may be able to take the initiative in developing the optical data bus as a strategic item. Japan's ground optical fiber communication technology, however, has so



far been developed with emphasis on long-distance, no-relaying, point-to-point data transmission technology. Even with the optical local area network (LAN), the active ring point-to-point system is the mainstream. It cannot be said, therefore, that studies have been sufficiently carried out for the short-distance light distribution technology, such as an optical data bus, for use in space. Further, optical fibers currently being used in space are step-index multimode fibers that are not generally used on the ground. It is necessary, therefore, to sufficiently acquire and evaluate basic data. As discussed below, the data bus carried by spacecraft requires light distribution technology. Development of the light distribution technology, therefore, must be positively carried out for use in space.

#### 4. Optical Data Bus Basic Structure

Optical fibers form a specific optical system for data transmission, rather than a harness. Unlike an electron data bus, optical fibers have peculiar difficulties in forming a network between data bus terminals (topology). There are topology classification concepts such as star, ring, and bus; topology can also be classified roughly into point-to-point type corresponding to active ring, and light distribution type using light branching couplers as shown in Figure 1. When these two types are compared for use in spacecraft, the light distribution type is more advantageous than the point-to-point type as a basic structure system for a space optical data bus, because of system reliability. These problems must also be studied from the standpoint of basic requirements for future spacecraft, such as network live wire extension during docking and fabrication on orbit.

#### 5. System Requirements for Future Spacecraft Use

Future spacecraft can be classified roughly into various types of space platforms and space shuttles. The major differences between these two are:

- Whether mission payloads are used.
- Whether there are changes in configuration on orbit due to operational replacement units (ORU), connection/separation between modules, etc.

Space platforms carry and use many items of mission payload and require high-speed, large-capacity data transmission. They also require high-speed, real-time command transmission for system control. Thus, the conventional electronic data bus exceeds the physical data transmission limit, and it is, therefore, indispensable to develop an optical data bus. In addition, to cope with on-orbit changes in configuration, and complicated operations, etc., involved in on-orbit service, it is necessary to develop a large number of new functions, etc., (including data bus) as a data processing system (Table 2). With respect to space shuttles, research on an optical data bus is being actively carried out, with consideration given to EMI resistivity, measures for thunderstorms, etc. It appears that future space shuttles having optical data buses will have many advantages.

	Example of typical formation	Effect of local failure on entire system
Point-to-point type		<ul style="list-style-type: none"> <li>• Terminal and bus line failures result in system down.</li> <li>• As measures for system down, the system is duplicated and bypass/loop-back functions are added. These measures, however, merely result in improvements almost equivalent to those of the light distribution type because it is necessary to use many optical switches.</li> </ul>
Light distribution type		<ul style="list-style-type: none"> <li>• Terminal and bus line failures do not extend to system down.</li> <li>• The light distribution system (star couplers, etc.) is passive equipment and highly reliable. Failures, however, result in system down, and appropriate measures such as duplicated installation, etc., must be taken.</li> </ul>

Figure 1. Point-to-Point Type and Light Distribution Type

## 6. Concepts on Research and Development

Figure 2 shows a structure of the data processing system including space optical data bus to achieve basic requirements for space platforms, etc., and Figure 3 shows the fields in which research subjects exist.

To achieve new functions such as on-orbit services, rendezvous docking, multimission, and autonomous control, it is necessary to study the following technological subjects required for a data bus.

### (1) Data Transmission/Control Technology

Functions of channel allocation change involved in the change of user mirror driving mechanism configuration. Flexible interequipment information exchange functions, such as linked operations of several subsystems (for example, manipulator and attitude control system, etc.), real-time HK data transmission to mission payload, and exchange of data between spacecraft after docking. Urgent and other data transmission control functions (based on priorities) involved in autonomous control functions of the data processing system.

Table 2. Basic Requirements for Data Processing System

- (1) User equipment configuration management/control technology
  - Change of dynamic automated channel allocation on orbit during operation
  - Study of on-board checkout functions and procedures on orbit during operation
 

ORU replacement/use and on-orbit fabrication/use are simply on-orbit integration. It is necessary, therefore, to study problems with data handling, such as work allocation between space and ground, etc., and checkout functions and procedures to be carried out at least in an on-board state, with regard to integration tests being currently carried out on the ground.
- (2) System reconfiguration management/control technology
  - Reconfiguration of the data processing system on orbit during operation
  - Network formation system for fabrication and separation on orbit during module formation and operation
  - Reconstruction of data networking between equipment carried by different spacecraft (during RVD) or different modules (during fabrication on orbit)
 

(For example, use of spacecraft A sensor data by equipment carried by spacecraft B, etc.)
- (3) Management and control technology between several subsystems
  - Management and control of linkage and coordination between several subsystems during advanced operations such as on-orbit services
  - Exchange of information between subsystems or equipment
- (4) System operation mode management and control technology
  - Changeover, establishment, and management of management/control mode per operation mode
  - System configuration management
  - Multimission payload operation management/control (status management, resource allocation, scheduling, etc.)
- (5) Abnormality management/control technology
  - Detection of abnormalities, and system-level management/control for moving to evacuation mode/involution mode
  - Redundancy management
- (6) Technology to cope with long-term operation, and development, and other advanced data transmission technology
  - Flexible/general data transmission technology to be able to comply with future unknown/unspecified mission payload requirements (Capable of handling a variety of data, flexibly changeable data transmission control, etc.)

[continued]

[Continuation of Table 2]

[Continuation]

- Advanced data transmission technology necessary for above management/control  
(For example, urgent/important data identification technology/preferential data transmission judgment technology, etc.)
- High-speed data transmission technology necessary to cope with multimissions and to support all above requirements
- Matching technology to cope with CCSDS and SODS

(7) Technology for interfacing with each subsystem and equipment

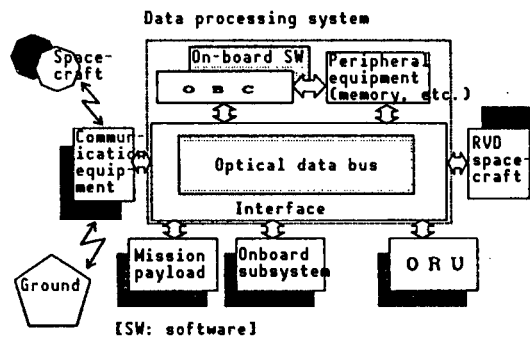


Figure 2. Data Processing System Structure

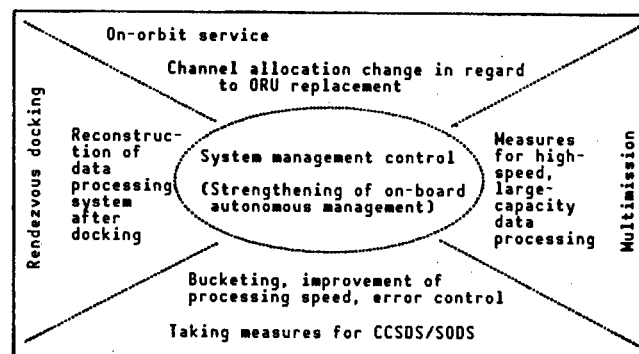


Figure 3. Field in Which Research Subjects Exist

(2) Data Bus Construction Technology Capable of Complying With Changes in Physical Configuration, Such as On-Orbit Fabrication and Docking Operation, and User Interface Technology

It is necessary to be able to easily and automatically separate and connect data bus construction on orbit when the data bus is in operation.

### **(3) System Management/Control Technology**

To comply with the maintenance/extension type replacement of equipment and changes in configuration on orbit, it is necessary to form a hierarchical structure, because a complex structure cannot be formed between several subsystems from both functional control and physical standpoints. The distributed control type, therefore, must be formed. To this end, supervisory control that coordinates controls between several subsystems while maintaining the integration of the entire spacecraft system must be carried out.

### **(4) Measures for Abnormal State (Autonomous Control)**

The diverse operations, such as rendezvous docking and increase of multi-mission payloads, will increase the possibility of hazardous conditions. It is necessary, therefore, to take appropriate measures for abnormal state (autonomous control) to maintain the minimal necessary system functions (in the on-board state).

## **7. Conclusion**

An optical data bus for use in space is not merely a data transmission system, but is the main point of the in-orbit spacecraft's central information system and must be constructed as an autonomous/multifunctional data processing system. With respect to data transmission/control technology, such as topology, access control system, various interfaces, and transmission protocol, it is necessary to study and develop the technology best suited to autonomous/multifunctional data processing system requirements. Further, light distribution/connection elements are the hub of an optical data bus. The success or otherwise of development of such elements appears to hold the key.

## **Fly-By-Light Element Technology Development**

906C3832E Tokyo HIKOKI SHINPOJIUMU in Japanese 18-20 Oct 89 pp 80-83

[Article by Mitsuyoshi Mayanagi, National Aerospace Laboratory]

[Text] 1. Introduction

Research and development (R&D) of fly-by-light for achieving an optical flight control system for aircraft has been actively carried out by overseas and domestic research institutes for more than 10 years. This R&D has addressed various types of sensors for detecting flight state volume, transducers for detecting mechanical positions (steering by pilot, steering angle on steering surface, etc.), data buses for data transmission, and actuators for driving steering surfaces.<sup>1-8</sup> These items of equipment, however, have not yet been put into practical use. To effectively carry out future work, it is necessary to recognize this R&D history.

In 1978, the National Aerospace Laboratory started research on fly-by-light as a part of research on the future STOL plane technology and has conducted research on optical transducers, optical data buses, and optical sensors at the laboratory level.<sup>9-11</sup> On the basis of achievements of this research, the laboratory has since 1983 conducted research on on-board type fly-by-light (FBL), aimed mainly at satisfying the requirements (small size, light weight, resistance to environment) for being carried by aircraft. So far, the laboratory has developed and manufactured (for experiments) on-board type optical transducers<sup>12</sup> and optical data buses,<sup>13</sup> and has conducted various evaluation tests.<sup>14-16</sup> The outline has already been reported.

This paper reports on these achievements and their current status, and clarifies the problems with FBL technology, with consideration given to future technological problems.

## 2. Status of FBL Element Technology

### (1) On-Board Optical Transducer<sup>12</sup>

This type of transducer (Figure 1 [not reproduced]) is composed of two transducers, four optical fiber cables, and one electronic interface unit (EIU), having the following major features.

- 1) The transducer portion is designed to be electrically passive (not using electricity), thus having superior resistivity to environments such as electromagnetic interference.
- 2) Serial optical digital signals are used as optical transducer outputs, thus aiming at simplifying the EIU connection hardware.

Table 1 presents the transducer performance. This transducer possesses an operating range of 360° and a 12-bit resolution (0.09°).

Table 1. Optical Transducer Performance

- |   |  |
|---|--|
| (1) Encoding part   |  |
| 1) Number of light source pulse receiving channels            | : 1  |
| 2) Number of light output signal transmission channels        | : 1  |
| 3) Number of light source pulse branches                      | : 14 channels  |
| 4) Each light pulse delay time                                | : 100 ns   |
| 5) Light delay line: quartz system, multimode fiber, NA: 0.25 |  |
| transmission loss   | : 10 dB/km, outside diameter : 300 $\mu$ m   |
| core/clad diameter  | : 80/125 $\mu$ m   |
| 6) Light output signal mode: series 14 bits (bit rate 10 MHz) |  |
| details: (synchronization: 1 bit,                             |  |
| data: 12 bits, parity: 1 bit)                                 |  |
| 7) Resolution   | : $2^{12} = 4096$ division   |
| 8) Accuracy   | : $\pm 0.5$ P (body), (after signal conversion:<br>$\pm 1$ P) P = $360^\circ/4096$ |
| 9) Speed of response  | : 10 kHz   |
| 10) Maximum allowable speed of rotation                       | : 3,000 rpm  |
| 11) Maximum allowable angle acceleration                      | : $10^5$ rad/sec <sup>2</sup>  |
| 12) Maximum allowable axial load                              | : radial direction: 20 N,<br>thrust direction: 10 N                                |
| 13) Starting torque   | : 8 N cm   |
| 14) Weight  | : 1 kg   |
| 15) Size  | : outside diameter 76 mm $\phi$ , length 135 mm                                    |
| 16) Light damping   | : 40 dBm   |
| 17) Environment resistivity: (based on MIL-STD-810 C)         |  |
| 1-Operating temperature                                       | : -54~+71°C  |
| 2-Temperature impact  | : (MIL-STD-810 C METHOD 503.1PROCEDURE 1)  |
| 3-Vibration   | : (equivalent to MIL-STD-810 C 514-2 H)  |
| 4-Impact  | : (equivalent to MIL-STD-810 C 514-2)  |
| 5-Tightness protection  | : altitude: equivalent to -15,000~+35,000<br>feet                                  |
| 6-Humidity  | : (equivalent to MIL-STD-810 C 507-1), less<br>than 95%                            |

[continued]

[Continuation of Table 1]

- |   |   |
|---|---|
| (2) Light source and signal processing part                                       |   |
| 1) Power supply   | : DC 28 V ( $\pm 6$ V)  |
| 2) Light source pulse generation and received signal processing                   | : time sharing system   |
| 3) Electricity/light conversion device: laser diode, output:                      | 30 mW   |
| 4) Light/electricity conversion device: photodiode, light receiving sensitivity : | $10^4$ V/W, rise time: 10 ns  |
| 5) Number of light source pulse transmission channels                             | : 2   |
| 6) Light source pulse transmission rate: Repetition cycle:                        | 20 $\mu$ s  |
|   | Pulse width : 50 ns   |
| 7) Time difference between light source pulse channels                            | : 10 $\mu$ s  |
| 8) Number of light signal receiving channels                                      | : 2   |
| 9) Light signal receiving bit rate:   | : 10 MHz  |
| 10) Number of digital signal output channels                                      | : 2   |
| 11) Number of digital signal output bits  | : 12  |
| 12) Digital signal output level   | : TTL level   |
| 13) Synchronization system: transmission/receiving synchronous processing system  |   |
| 14) Number of analog signal output channels: 2 (for use in monitors)              |   |
| 15) Analog signal output mode   | : $\pm 10$ V  |
| 16) Weight  | : less than 6 kg  |
| 17) Size (length x width x depth)   | : 205 x 126 x 320 mm  |
| 18) Environment resistivity   | : (based on MIL-STD-810 C)  |
| (3) Transmission/receiving optical fiber code                                     |   |
| 1) Material   | : quartz system, multimode fiber  |
| 2) Characteristics: NA  | : 0.21, transmission loss: 15 dB/km   |
| 3) Dimensions   | : outside diameter: 2.0 mm, length: 20 m<br>core/clad diameter: 500/610 $\mu$ m |
| 4) Environment resistivity:   | Same as those given in (1) and (2) above  |

This transducer has to date been developed in the following three stages.

- 1) Initial development
- 2) Improvement of strength resistible to vibration tests
- 3) Development involved with improvement of optical output signal S/N

Initial developments used parallel light for transmission to maintain the required fabrication accuracy and facilitate fabrication, adjustment, etc. As a result, several problems occurred in the S/N characteristics of optical output signals, as shown in Figure 2(a) [not reproduced] and improvements were expected. The second development was carried out to improve the mechanical strength of the transducer concerned, because it was broken during vibration tests. A dummy was manufactured and tested to confirm the strength. The results of tests were incorporated in the later manufacture of transducers. Further, the improvement of S/N characteristics expected in the first development was carried out by using focused light for transmission.



As a result, the required mechanical strength was obtained, but bits not output occurred in part of the optical output signal. This problem, however, was expected to be resolved by improving the transmission light receiving structure (adjustable structure), enhancing manufacturing accuracy, and selecting parts (unification of quality). The third development, therefore, was carried out. Consequently, the newly developed transducer was able to greatly improve the S/N characteristics, compared with the initially developed one as shown in Figure 2(b) [not reproduced]. As a result of tests, the initially developed EIU involved problems with on-board environments in regard to power supply noise and laser diode temperature characteristics. The former is not an essential problem and can be resolved by conventional technology. To resolve the latter problem, it has become necessary to develop new EIUs satisfying the on-board environment condition or to carry out temperature control. The later developments on these problems, however, remain suspended.

## (2) On-Board Optical Data Bus<sup>13</sup>

As shown in Figure 3 [not reproduced], this optical data bus system is composed of a central arithmetic processing unit, input terminal, output terminal, and light transmission part that connects each unit. The light transmission part incorporates a pressurized partition wall, multicore optical connector, with consideration given to the case of equipping for practical use; it is composed of an optical star coupler, light transmission/receiving unit, single core light connector, and optical fiber cables.

This optical data bus uses the command response and time sharing multiplex data transmission system based on optical data bus standard DOD-STD-1773<sup>17</sup> being proposed in the United States. Further, a power transmission line is provided as a backup system during failure of the optical transmission line.

The optical data bus performance is given in Table 2, except for the light transmission part. The optical data bus performance falls within the range of electronic data bus standard MIL-STD-1553 A and B,<sup>18</sup> as each item given in Table 2 shows. The light transmission part performance is given in Table 3. The damping of light has a maximum of 19.96 dB and a minimum of 15.14 dB, respectively, except for the light transmission/receiving unit. This range can be fully coped with by currently available technology.

No data transmission errors have occurred in the environment tests,<sup>14</sup> ground performance evaluation tests<sup>15</sup> (30 times, 200 hours), and flight tests<sup>16</sup> (10 times, 15 hours) so far conducted.

Table 2. Optical Data Bus System Performance

(1) Optical data bus		
1) Bus control system	: command response system (CCB system)	
2) Terminal control system	: microprogram system	
3) Transmission system		
1-Encoding system	: Manchester code	
2-Word length	: 20 bits/word	
3-Word mode	: synchronization (3) + data (16) + parity (1)	
4-Type of words	: command, status, data	
5-Transmission speed	: 1M bits/s	
6-Number of data words	: 32 words	
4) Data transmission direction		
1-Central arithmetic processor (BC)→input/output terminal (RT)		
2-Input/output terminal (RT)→central arithmetic processor (BC)		
3-Input/output terminal (RT)→input/output terminal (RT)		
5) Mode command	: based on MIL-STD-1773	
6) Transmission cable		
1-Optical fiber cable (maximum length 80 m)		1 ch
2-Electric cable (maximum length 30 m)		1 ch
(2) Input/output signal to outside		
1) Central arithmetic processor		
: Discrete input/output signal (D I/O)		8/8 ch
: Analog input/output signal ( $\pm 10$ V), (AI)		10 ch
2) Input terminal		
: Discrete input/output signal (DI/O)		56/24 ch
: Arinc input/output signal (ARINC I/O)		2/1 ch
3) Output terminal		
: Discrete input/output signal (D I/O)		24/10 ch
: Analog input/output signal ( $\pm 10$ V), (AI/O)		7/3 ch
: Arinc input/output signal (ARINC I/O)		1/1, (1/0) ch
4) Each equipment: PC-9801 input/output signal (RS-422)		1 ch
(3) Board common to CPU and BIU		
1) CPU ROM: 32 kW, RAM: 8 kW (BC: addition of ROM (64 kW)		
2) CPU clock: 5 MHz		
3) BIU buffer RAM: 4 kW (1 W: 16 bits)		
(4) Dimensions and weight of each equipment:		
(126) w x (193) h x (319) d, 10 kg		
(5) Power supply (common to each equipment): DC 28 V ( $\pm 1_6$ V), 3A		
(6) Environment resistivity: Performance that can pass tests based on MIL-STD-810 C and MIL-STD-461A CLASS A1		

Table 3. Light Transmission Part Performance

(1) Optical fiber	
1) Type	: Quartz step index multimode fiber
2) Core diameter	: $100 \pm 5 \mu\text{m}$ , clad diameter: $140 \pm 5 \mu\text{m}$
3) NA	: $0.27 \pm 0.02$
4) Outside diameter	: about $1.5 \text{ mm}\phi$
5) Casing	: fluorine resin, primary coating: silicon resin
6) Tension member	: polyester resin
7) Transmission loss	: 7 dB/km or less (wavelength $0.85 \mu\text{m}$ )
8) Transmission band	: 10 MHz km or more (wavelength $0.85 \mu\text{m}$ )
9) Length	
1-No. 1 optical fiber	: 10 m x 6
2-No. 2 optical fiber	: 20 m x 2, 10 m x 2
3-No. 3 optical fiber	: 20 m x 4
(2) Light transmission/receiving unit	
1) Transmission route	: 2M bits/s (NRZ)
2) Power supply:	: +5 V, -15 V
3) Optical connector	: Can be connected to type FC
4) Light-emitting device	: LED, output: 1 mW, wavelength: $0.85 \mu\text{m}$ Optical signal transmission level: -10 dBm or more
5) Light-receiving device	: Silicon PIN photodiode Optical signal minimum receiving level: -32 dBm or less
(3) Light branching connector	
1) Optical star coupler	: 1
1-Light branching connection system	: mixing rod, transmission system
2-Number of input/output boards	: 16 ch (No. of packaged pins: 6)
3-Insertion loss	: within 15 dB (including connector loss)
4-Light distribution deviation	: within 2 dB
5-Optical multicore connector	: 16 cores (pin #20)
6-Dimensions, weight	: $125 \times 85 \times 35 \text{ mm}$ , 800 g or less
2) Pressurized partition wall optical connector (4 cores, pin #20)	: 1
• Insertion loss	: within 1.5 dB (loss of both types of connectors)
3) Multicore (a) optical connector (16 cores, pin #20)	: 1
4) Multicore (b) optical connector (4 cores, pin #20)	: 2
5) Optical single core connector (can be connected to type FC)	: 14
• Insertion loss	: within 0.7 dB (during adapter use)
6) Optical single core adapter (can be connected to type FC connector)	: 4
(4) Total of light transmission part transmission loss:	
• Maximum	: $1.5 \times 2 + 0.7 \times 2 + 15 + 7 \times 0.08 = 19.96 \text{ dB}$
• Minimum	: $15 + 7 \times 0.02 = 15.14 \text{ dB}$

### 3. Problems With FBL Technology

#### (1) On-Board Optical Transducer

The following items can be cited as problems with the on-board optical transducers. Most of these problems arise from the use of existing optical components.

- 1) Miniaturization of optical transducer
- 2) Reduction of optical path composing element optical power attenuation
- 3) Equalizing of each optical delay pulse power
- 4) Reduction of starting torque
- 5) High-speed timing clock generation circuit
- 6) Laser diode temperature characteristics

#### (2) On-Board Optical Data Bus

No particular problems can be cited for the optical data bus. It should be noted, however, that breaking of wires occurred once at the connector portion during the setting up of environment tests and once during laboratory-level tests. Care, therefore, must be fully taken in handling optical fiber codes. It appears necessary to establish rules that only qualified personnel handle optical fiber codes.

### 4. Problems With FBL Element Technology and Future Prospects

#### (1) Problems With On-Board Optical Transducer

- 1) Development of optical delay fiber accounting for about half of optical transducers.
- 2) Improvement of light source pulse rate and development of high-speed timing clock generation circuit.
- 3) Development of optical path composing element (particularly, transmission/receiving head adaptable to slit).
- 4) Development of starting torque reduction seal technology.
- 5) Development of laser diode satisfying on-board temperature conditions.

#### (2) Problems With On-Board Optical Data Bus

- 1) Development of high-speed data transmission technology, one of the advantages in optical data transmission.
- 2) Development of high-speed signal processing technology.

### (3) Future Prospects for FBL Technology

In view of data transmission tests (several G bits/s) conducted in the latest optical communication field, development of high-speed (10-20 GHz) LSI package, etc., it appears that optical signals can be easily transmitted at high speed in the near future and that the sufficient utilization of the advantages of light will serve to further proceed with the practical use of FBL technology.

### 5. Conclusion

Research on on-board FBL elements has been conducted for many years as a part of research and development on future STOL aircraft technology. The research, however, is scheduled to be completed in 1990.

On-board optical transducers were manufactured and developed for experiments while several problems were being resolved. Prospects for practical use, however, were obtained.

The trial development and manufacture of on-board optical data buses was carried out without specific problems. Various tests on the ground were completed, and flight tests are currently being carried out. It appears necessary to develop fly-by-light control systems that allow flight tests to be carried out using actual aircraft, and thereby to establish reliability and prove practicality.

### References

1. Mayanagi, M., "Optical System for Aircraft," OPTOELECTRONICS, April 1983.
2. "Investigation of Technical Trend in Fly-By-Light," Japan Aerospace Industry Society, 1983.
3. Mayanagi, M., "Optical Technology for Flight Control System," JAPAN AEROSPACE ACADEMIC SOCIETY JOURNAL, Vol 32 No 369, October 1984.
4. Fox, E.V., Jr., "Fly-By-Light: The Sensors, A Key System Element," AIAA/IEEE Fourth Digital Avionics Systems Conference, 17-19 November 1981.
5. Seymour, N.L., "Evolution of an Optical Control System for Aircraft Hydraulics," SAE TECHNICAL PAPER Series 801195, October 1980.
6. Shaunfield, J.E. and Blard, J.R., "An MIL-STD-1553 Fiber Optic Data Bus," AFSC Multiplex Data Bus Conference, November 1976.
7. Anderson, J.D., et al., Fiber Optic Data Bus, 1977.

8. Harder, R.D., Greenwell, R.A., and Holma, G.M., "A-7 Airborne Light Optical Fiber Technology (ALOFT) Demonstration Project," NELC TECHNICAL REPORT, No 2024, February 1977.
9. Mayanagi, M., "Optical Pulse Digital Transducer," 20th SICE Academic Lecture Meeting Preliminary Draft Series, July 1981.
10. Ibid., "Trial Manufacture of Optical Pulse Digital Transducer," 26th Automatic Control Lecture Meeting, November 1983.
11. Mayanagi, M., et al., "R&D of Aircraft Optical Fiber Data Bus (I) System Structure and Basic Design (II) Bus Control," 20th Aircraft Symposium Lecture Series, November 1982.
12. Mayanagi, M., Takizawa, M., Uchida, T., Ebara, Y., and Hoshikawa, M., "Trial Manufacture and Development of Digital Optical Rotary Position Transducer," SYSTEM AND CONTROL, Vol 32 No 5, April 1988.
13. Mayanagi, M., et al., "On-Board Optical Data Bus (I) Trial Manufacture and Development," 26th Aircraft Symposium Lecture Collection, October 1988.
14. Takizawa, M., et al., "On-Board Bus (2) Environment Tests," 26th Aircraft Symposium Lecture Series, October 1988.
15. Mayanagi, M., et al., "On-Board Optical Data Bus (3) Bus Control Software and Performance Evaluation Test," 27th Aircraft Symposium Lecture Series, October 1989.
16. Uchida, et al., "On-Board Optical Data Bus (4) Flight Test," 27th Aircraft Symposium Lecture Series, October 1989.
17. "Proposed DOD-STD-1773: Fiber Optics Mechanization of an Aircraft Internal Time Division Command/Response Multiplex Data Bus," April 1985.
18. U.S. Department of Defense: MIL-STD-1553 A,B Aircraft Internal Time Division Command/Response Multiplex Data Bus, 1975, 1978.

## **Application of Optical Communication Parts to Optical Data Bus**

906C3832F Tokyo HIKOKI SHINPOJIUMU in Japanese 18-20 Oct 89 pp 84-87

[Article by Takeshi Sugawa and Yasunori Murakami, Sumitomo Electric Industries, Ltd.]

### **[Text] 1. Introduction**

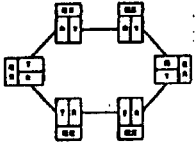
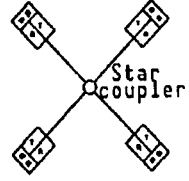
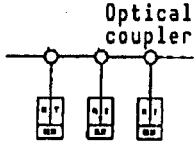
Full-scale research and development of optical communication technology started in 1970 and has made marked progress. The practical use of such technology has so far been widely studied in regard to communication/control systems for use in electrical industries, traffic, computers, industrial plants, etc., as well as long-distance communications. Optical communications are the mainstream of long-distance communications. Further, the optical communication network (optical LAN), within the limited area represented by industrial plants and computer communication networks, has reached the practical use stage. Under such circumstances, the application of optical communication technology to extremely limited space such as one plant or aircraft is being attempted. The use of an optical data bus is thought to ensure construction of the most simple communication network. This paper, therefore, describes the optical data bus and the current status of development of optical communication parts composing a data bus.

### **2. Optical Communication Network Structure**

As major optical communication network structures composing closed networks such as optical LAN, three types can be cited: ring, star, and linear bus types (Table 1).

The ring type is suitable for large-capacity optical networks requiring a signal transmission speed of 100 Mb/s or more and requires the use of high-speed light transmitters/receivers as optical communication parts. In some cases, to improve the reliability of the network, circuits are protected using light switches. The star type is suitable for medium-capacity optical networks requiring a signal transmission speed of several 10 Mb/s. The structure is comparatively simple and reliability is high. The use of star couplers, however, causes optical fibers to be congested in the vicinity of the star coupler, thus posing problems with system layout and maintenance. The linear

Table 1. Classification of Optical Communication Network

	Ring type	Star type	Linear bus type
Capacity	Large Several 100 Mbps	Medium Several 10 Mbps	Small Several Mbps
Features	Small wiring volume	High reliability	Easy laying
Problems	Reliability	Wiring volume	Number of connection terminals
Structure	 <p>T: light transmitter R: light receiver</p>	 <p>T: light transmitter R: light receiver</p>	 <p>T: light transmitter R: light receiver</p>

bus type is comparatively small in communication capacity but is composed of passive parts, thereby resulting in highly reliable networks that ensure ease of layout and maintenance. For application to the inside of aircraft, the linear bus type appears to be desirable. In such networks, however, the light transmission/receiving performance and optical coupler performance cause the signal transmission speed and number of connection terminals to be limited. Using optical communication parts so far developed, we formed a linear bus type network and evaluated the performance. Figure 1 shows a structure of the linear bus type network studied.

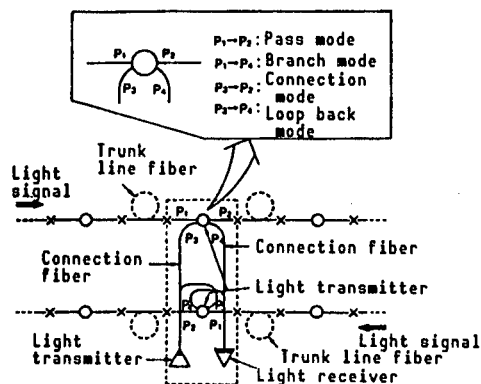


Figure 1. System Structure



With respect to trunk lines, one optical fiber was used for the upward line and one for the downward line. Part of the light signals propagating in the trunk line is branched at a light tap, consisting of a light coupler, and is connected at each terminal. Therefore, a high efficiency in coupling to the trunk line optical fibers and a low branch efficiency to prevent the deterioration of propagating light signal level, as well as low insertion loss, are required for light couplers. Regarding light signal transmitter-receivers, the difference in light level between transmission and receiving must be large, and the light receiving dynamic range must be wide in order to increase the number of terminals. Further, to enhance the efficient use of circuits, light transmitter-receivers must be able to receive light signals from the first bit. It is also necessary that the light receiver recovery time (time required until the light receiver can receive weak light signals immediately after receiving strong light signals) be short.

### 3. Light Signal Level Design

As mentioned above, the optimum design of light level is thought to play an important role in achieving the practical use of the linear bus type network. Performance necessary for light couplers was calculated for the cases where the differences in the level between light transmission and receiving are 30 dB and 35 dB and where the number of connection terminals are 30, 50, and 70. The results are shown by the solid lines in Figure 2. The performance of light couplers so far used in optical communications (symmetrical light coupler = optical fiber, in which the trunk line and branch lines are the same type of optical fibers) is as shown by broken lines. In other words, it is known that the conventional light couplers cannot be formed as a system.

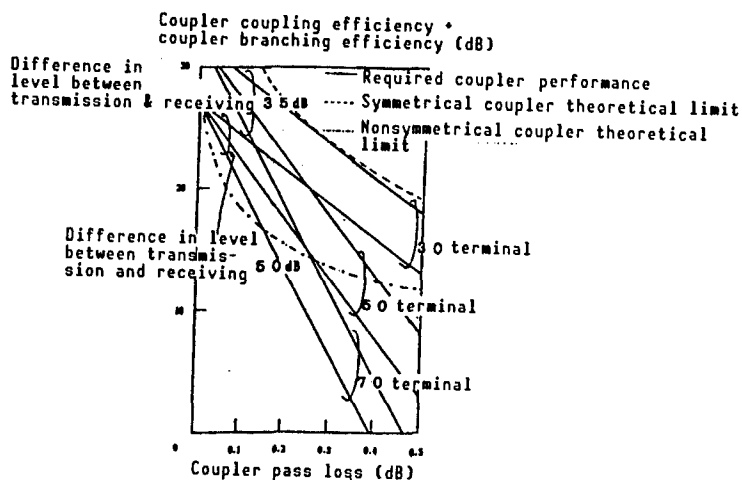


Figure 2. Number of Connection Terminals and Required Coupler Performance

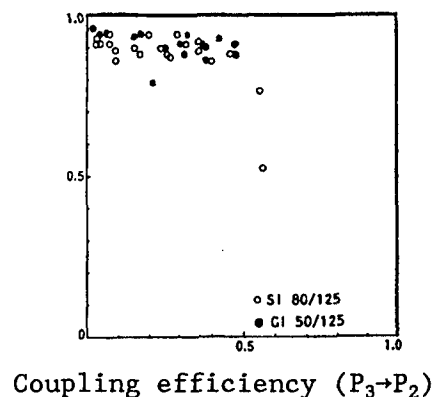


Figure 3. Comparison of Unsymmetrical Coupler Performance

To solve the above problem, it appears necessary to use nonsymmetrical couplers, in which optical fibers each having a large core diameter and a high NA are used for trunk lines, and those having a small core diameter and a low

NA are used for branch lines. Therefore, using 208/250  $\mu\text{m}$  ( $\text{NA} = 0.36$ ) optical fibers for trunk lines and two types of optical fibers for branch lines, light couplers were manufactured on a trial basis and the results shown in Figure 3 were obtained.

The theoretical limit in cases where the couplers made of the above optical fibers are used, is as shown in Figure 2 with alternate long and short dash lines. In view of only optical level design, it appears that the couplers can connect 70 or more terminals. On the basis of this optical level design, the target performance of light couplers and light transmitter-receivers has been arranged as per Table 2 to maintain the number of connecting terminals at 50 or more.

Table 2. Target Performance of Optical Parts

Name of optical parts	Requirements		
Light coupler	Low pass loss	$(P_1 \rightarrow P_2)$	$<0.15 \text{ dB}$
	High coupling efficiency	$(P_3 \rightarrow P_4)$	$<20 \text{ dB}$
	Low branching efficiency	$(P_1 \rightarrow P_4)$	(sum)
	High loop-back loss	$(P_3 \rightarrow P_4)$	$>10 \text{ dB}$
Light signal transmitter-receiver	Transmission speed	2 Mbps	
	High coupling power	$>30 \text{ dB}$	
	High receiving sensitivity	(difference in level)	
	High dynamic range	$>20 \text{ dB}$	
	Fast recovery time	$<0.2 \mu\text{s}$	

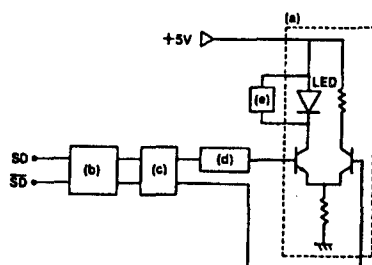
Light coupler pass loss, coupling efficiency, branching efficiency, and differences in level between signal transmission and receiving are values determined based on Figure 2. Further, it is designed so that the sum of the coupler loop-back loss and the transmitter-receiver dynamic range becomes the same as differences in level between light transmission and receiving.

#### 4. Development of Element Parts

##### 4.1 Light Transmitter

A light transmitter was manufactured on a trial basis using an LED (central light emitting wavelength: 850 nm, spectrum width: 60 nm) as a light source. The structure of the light transmitter is shown in Figure 4. Changes in LED emitting power arising from temperature and power supply fluctuations were stabilized, input signal pulse width distortion was compensated, and a circuit to shorten the light pulse rise/decay time was added. Thus, attempts were made to achieve the targets given in Table 2. As a result, a light coupling power of  $-3 \text{ dBm}$  (peak value) was obtained for 80/125  $\mu\text{m}$  fibers. Further, the LED emitting power fluctuations have been controlled to 0.4 dB with respect to

temperature fluctuations from  $-20$  to  $70^{\circ}\text{C}$  and a power supply fluctuation of  $5\text{ V} \pm 10$  percent, as shown in Figure 5.



- (a) Differential transistor circuit for LED driving
- (b) Light pulse width compensation circuit
- (c) Light emitting power stabilization circuit
- (d) Light pulse rising time compensation circuit
- (e) Light pulse decaying time compensation circuit

Figure 4. Light Transmitter Block Diagram

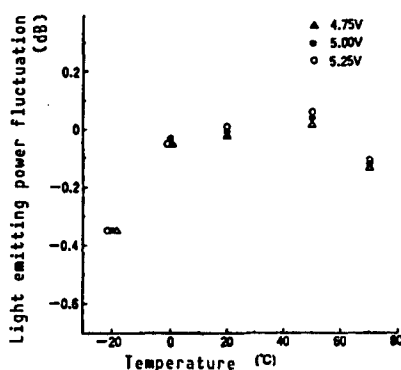
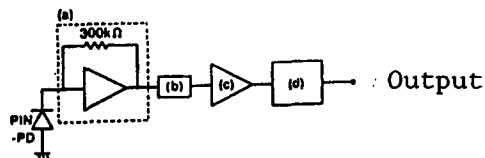


Figure 5. Light Coupling Power Variation  
(Coordinates at  $20^{\circ}\text{C}$  and  $5.00\text{ V}$  were assumed to be 0.)

## 4.2 Light Receiver

A light receiver as shown in Figure 6 was manufactured on a trial basis using an  $0.8\text{ }\mu\text{m}$  band Si-PIN photodiode.



- (a) Trans-impedance preamplifier
- (b) Differentiating circuit
- (c) Main amplifier
- (d) Signal identification circuit

Figure 6. Light Receiver Block

Using an all-stage DC connection amplifier, a trans-impedance amplifier was constructed. Thus, the light receiver could receive even signal bursts from the first bit, and a function capable of correctly identifying the silence condition was achieved. The sensitivity of the unit receiver capable of receiving 2 Mb/s Manchester signals from the first bit was -41 dBm. The recovery time of the light receiver is as given in Table 3.

Table 3. Light Receiver Recovery Characteristics

Weak optical signal (dBm)	Strong optical signal (dBm)					
	-15	-20	-25	-30	-35	-40
-20	<2 $\mu$ s	<2 $\mu$ s	—	—	—	—
-25	<2 $\mu$ s	<2 $\mu$ s	<2 $\mu$ s	—	—	—
-30	<2 $\mu$ s	<2 $\mu$ s	<2 $\mu$ s	<2 $\mu$ s	—	—
-35	<2 $\mu$ s	<2 $\mu$ s	<2 $\mu$ s	<2 $\mu$ s	<2 $\mu$ s	—
-40	14.5 $\mu$ s	10.9 $\mu$ s	<2 $\mu$ s	<2 $\mu$ s	<2 $\mu$ s	<2 $\mu$ s

As given in Table 2, a time of <2  $\mu$ s was required to return to the state in which weak light signals (-35 dBm) can be properly received after the receiving of strong light signals (-15 dBm) was completed. The sensitivity of a practical light receiver in this system is thought to be -35 dBm and the dynamic range of to be 20 dB.

#### 4.3 Light Coupler

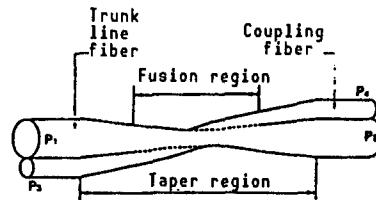
On the basis of the said level design, a light coupler was manufactured on a trial basis using optical fibers given in Table 4.

Table 4. Optical Fiber Parameters

Optical fiber	Core diameter	Core Specific refractive index	Clad diameter	Clad Specific refractive index
Trunk line optical fiber	208 $\mu$ m	2.6%	250 $\mu$ m	-1%
Coupling optical fiber	80 $\mu$ m	1%	125 $\mu$ m	-1%

Note: Specific refractive ratios are values obtained by comparing optical fibers with pure quartz

To achieve low loss, the fusion taper system shown in Figure 7 was employed. In addition, the coupling optical fiber clad refractive index was reduced by fluorine doping. As a result, the excessive loss was 0.06 dB, as given in Table 5 below.



Note:  $P_1 \rightarrow P_2$  pass mode  
 $P_1 \rightarrow P_4$  branch mode  
 $P_3 \rightarrow P_2$  coupling mode  
 $P_3 \rightarrow P_4$  loop back mode

Figure 7. Light Coupler

Table 5. Results of Trial Manufacture

Pass loss ( $P_1 \rightarrow P_2$ )	Coupling loss ( $P_3 \rightarrow P_2$ )	Branching loss ( $P_1 \rightarrow P_4$ )	Loop loss ( $P_3 \rightarrow P_4$ )	Excessive loss
0.14 dB	2.07 dB	17.23 dB	10.46 dB	0.06 dB

The trunk line optical fiber connection loss arising from the slave connection of light couplers can be calculated to be 0.15 dB on average, due to the scattering (in manufacturing) of trunk line optical fiber core diameter and clad diameter. The calculations show that a combination of the aforesaid light transmitter-receiver performance and the light coupler performance makes it possible to connect 57 terminals.

## 5. Conclusion

The use of the linear bus network was studied to achieve a low-speed simple network. The study has revealed that the use of low-loss nonsymmetrical light couplers and high power budget, a complete DC connection light transmitter-receiver may be able to connect 50 or more terminals in view of the level design. It should be noted, however, that aircraft having requirements different from those of general communication systems require the development of different element parts and require studies including system and reliability design.

## R&D of Passive Optical Gyro

906C3832G Tokyo HIKOKI SHINPOJIUMU in Japanese 18-20 Oct 89 pp 88-91

[Article by Kazuo Hotate and Minoru Higashiguchi, High Scientific Technology Research Center of Tokyo University]

### [Text] 1. Introduction

This paper describes the trend in the research and development of optical fiber gyros. Coherent optical fiber gyros have recently made marked progress and are reaching the stage of precipitation. Further, basic research is being conducted on passive ring resonance gyros. The use of short optical fibers makes it possible to manufacture highly sensitive passive ring resonance gyros, and this is receiving much attention.<sup>1-11</sup>

### 2. Classification and Features of Passive Gyros

Passive optical gyros can be classified into coherent optical fiber gyros and optical passive ring resonance gyros (OPRG), as shown in Figure 1 below.

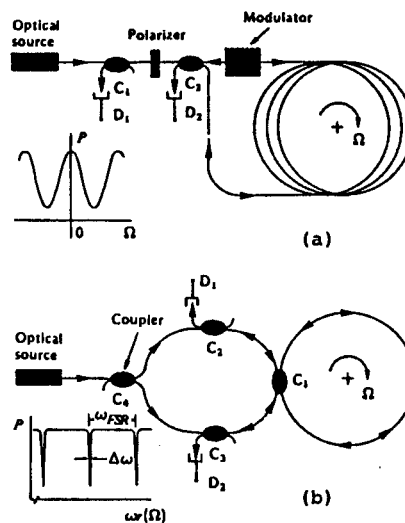


Figure 1. Passive Optical Gyro Structure

In the case of coherent optical fiber gyros, lengthy optical fibers (for example, 1 km) are wound with a comparatively small diameter (for example, 2.5 cm), as shown in Figure 1(a), thus aiming at improving the sensitivity by twice the number of winds (6,300 times). Measurement of interference of two lights turning and propagating (in the sensing loop) in the opposite direction to each other makes it possible to form a gyro. A resolution of about 0.02 deg/h and zero point stability have already been achieved. A scale factor stability of about 30 ppm has also been obtained, and products have already been put on the market.

OPRGs form a ring-shaped optical resonator that has a high fineness ratio and achieve changes in resonance frequency arising from Sagnac effects. The sensitivity can be improved by twice the fineness ratio, thereby making it possible to manufacture short optical fibers. A trial calculation indicates that the inertial navigation grade can be achieved by a fiber length of less than 10 m. Although OPRGs are still in basic research, many hopes are placed on their future practical use.

Even the above passive optical gyros have a frequency output, as in the case of ring laser gyros. As a result, they can achieve a wide dynamic range and are receiving attention as strap-down gyros. These passive type optical gyros have no moving parts, thus rapidly improving their ease of use. New applications, therefore, are expected to be developed.

### 3. Coherent Optical Fiber Gyro

To be used for aircraft, optical fiber gyros must be able to measure changes ( $\mu$ rad) in light wave phase. It is indispensable, therefore, to take appropriate measures for noise factors.<sup>3-6</sup> Research on such measures can be said to have been completed in regard to coherent optical fiber gyros. Understanding the behavior of major noise factors—such as optical kerr effects in optical fibers, temperature distribution fluctuations, polarization fluctuations, Rayleigh scattering, and effects of earth magnetism—and measures to be taken for these noise factors, have been fully devised.

For example, geomagnetism causes optical fibers to operate as a Faraday device, thereby resulting in drifts corresponding to the rotation of the earth. The author, et al., have shown that it is possible to reduce such drifts by using polarized wave-maintaining optical fibers.<sup>12,13</sup> Further, we have theoretically and experimentally made clear that these drifts occur solely when a torsion component, in which one turn of an optical fiber loop is established to be one cycle, exists.<sup>13</sup> Twisting of optical fibers with only plate FBI, shown in Figure 2(a), causes the above torsion component to be produced and thereby results in the torsion becoming half the above cycle and only its higher harmonics. As a result, the bias is rectified.<sup>13</sup>

In other words, the removal of torsion completely eliminates the need for magnetic shielding.

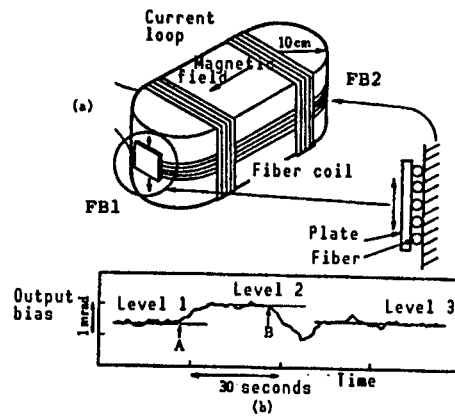


Figure 2. Repression of Faraday Effect Induction Noise by Removing Special Torsion Component<sup>13</sup>

On the basis of the above basic research, a resolution of 0.02 deg/h and zero-point stability were obtained using the phase modulation process (a comparatively simple construction), and were made public. Since then, data equivalent to the above resolution and zero-point stability have been obtained at various research institutes.<sup>4-6</sup> Figure 3 shows data recently obtained. From this figure, it can be shown that resolutions close to the theoretical limit have been achieved.<sup>14</sup> In addition, a scale factor stability of about 30 ppm was achieved.<sup>14</sup> Thus, the phase modulation process is becoming a fully completed technology, although it must achieve the dynamic range. In the United States, gyro manufacturers or users have recently made public superior prototypes.<sup>6,15</sup> Similar trends can be seen in Japan.<sup>11</sup> Further, several firms have started selling medium-size models.

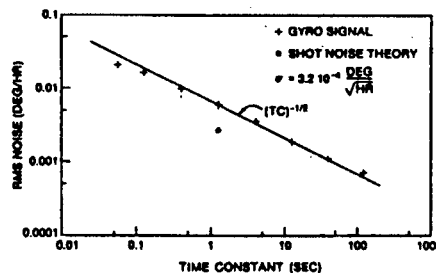


Figure 3. Characteristics of Phase Modulation System Optical Fiber Gyro<sup>14</sup>  
(Noise was extremely repressed.)

Signal output at frequencies equivalent to that of ring laser gyros are indispensable to substantially enlarge the dynamic range. Processes capable of achieving such signal output, include optical heterodyne process fiber gyro,<sup>16</sup> frequency change process, and serrodyne process. The serrodyne process is thought to have resulted from improvement of the frequency change process.<sup>4-6</sup>

Of the above processes, the digital serrodyne process is receiving much attention. An example of its composition is shown in Figure 4(a).<sup>17</sup> A step voltage, shown in Figure 4(b-1), is superimposed on the phase modulator.



(a)

(1)

(2)

(3)

(b)

- (b-1) Phase modulation waveform
- (b-2) Difference in phase between left/right lights
- (b-3) Light receiver output<sup>17</sup>

The above process allows frequency output to be obtained with the same structure as that of the optical system of the phase modulation process, which has so far been superior in resolution and zero-point stability. This process not only resolves dynamic range problems, but also serves to stabilize scale factors because this process is a zero method construction. It is necessary to use waveguide optical phase modulators that are fully superior in frequency characteristics. Phase modulators are of a construction in which  $T_i$  is

dispersed on an x-cut  $\text{LiNbO}_3$  substrate.<sup>18</sup> Optical devices using  $\text{LiNbO}_3$  have so far involved problems in temperature stability. This digital serrodyne system, however, can compensate the above device characteristics by means of double feedback loops located in the gyro system and can be said to be an excellent invention.

The Litton Co., in the United States, has recently achieved the following performance<sup>17</sup>:

- Random walk:  $0.005^\circ/(\text{hour})^{1/2}$
- Resolution :  $0.01^\circ/\text{hour}$
- Scale factor stability: 100 ppm or less

As shown in Figure 5, the dynamic range is seven-digit numbers. Thus, the system has already obtained an overall performance worthy of use for aircraft inertial navigation. There is a high possibility that this system will become a highly efficient coherent optical fiber gyro.

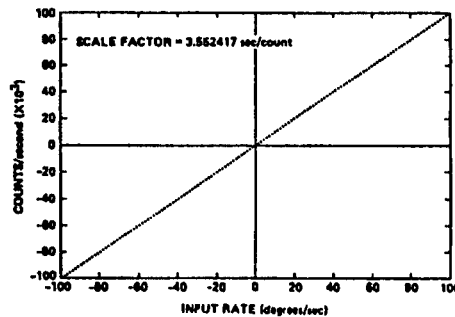


Figure 5. Digital Serrodyne Optical Fiber Gyro Characteristics<sup>17</sup>

#### 4. Passive Ring Resonant Optical Gyro

Passive ring resonator length fluctuates according to temperature and mechanical factors. To offset the effect of this fluctuation, it is necessary to use light turning left and right. The system shown in Figure 1(b) becomes a basic optical system. It is still necessary, however, to grasp the behavior of various noise factors in regard mainly to zero-point stability.<sup>19</sup> The results of studies so far conducted are presented in Table 1.<sup>4-6</sup> As shown in Table 1, many noise factors have already been studied.

OPRGs use the resonance of light and require a highly coherent optical source, unlike optical fiber gyros. In other words, it is necessary to study an optimum relation between each parameter of the optical source coherence and resonators, and to make clear the theoretical sensitivity limit obtained by such study. Using the optical source spectral width as parameters, the OPRG theoretical rotating detection limit was analyzed as a function of length of optical fibers composing optical resonators. The results of such analysis<sup>20</sup> are shown in Figure 6. It can be shown that the fibers have optimum length and that this optimum length is several meters to several tens of meters.

Table 1. Passive Ring Resonant Optical Gyro Performance  
(Restrictive factors and measures to be taken)

Noise factor	Explanation	Measures
Optical source coherence	Extraction of sharp resonance characteristics requires a narrow spectral optical source: Spectral width; 10~100 kHz	It is necessary to change semiconductor laser beams into narrow spectrums.
Polarization state fluctuation in optical fiber	Two peculiar polarization states exist in a ring resonator, and it is necessary to excite only one state.	Use of two-polarization state adjustor: Required adjusting accuracy is extremely high. Polarized wave maintaining optical fibers are used.
Uneven temperature fluctuations in optical fibers	Uneven optical fiber temperature fluctuations in the longitudinal direction result in changes in output.	Optical fibers are wound in such a way as to obtain a temperature distribution symmetrical with respect to the center of the optical fibers. (The optical length is shorter compared with the coherent system type, and there are no large effects of uneven temperature fluctuations.)
Optical kerr effects in optical fiber due to propagating light strength	Optical kerr effects due to the strength of light propagating in optical fibers becomes a contribution of 1:2 for light turning in the direction reverse to itself. Consequently, changes in the distribution ratio of directional couplers cause output to change.	The optical source is modulated using square waves of 50 percent in duty.

[continued]

[Continuation of Table 1]

Noise factor	Explanation		Measures
Backward Raleigh scattering in optical fiber	Backward scattering having occurred in a resonator forms two components on a light receiver. These two components show resonance characteristics: coherent component of signal light and scattering light, strength of scattering light.	The former vibrates at a frequency in proportion to input rotation in the system having feedback to incident light wave frequency, thereby causing a lock-in phenomenon.	Carrier frequency is removed by applying PM or FM to light turning right or left.
		The latter shows bipeak characteristics during turning input, causing deterioration of linearity.	Light turning left and right at a different frequency undergoes Pm or FM, and the light receiver outputs are synchronized and demodulated. Thus the resonance peak of signal light is obtained.
Geomagnetic	Geomagnetic causes optical fibers to operate as a Faraday device, thus giving differences in resonant frequency between light turning left and right, coupled with the retarder mechanism in optical fiber.		Special torsion components are removed using polarized wave maintaining optical fibers.

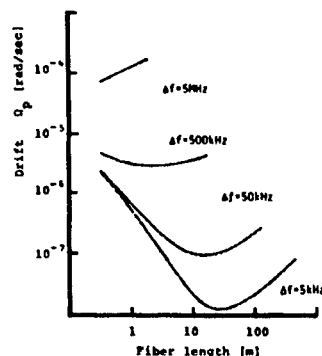


Figure 6. Theoretical Rotating Detection Limit of Passive Ring Resonance System Optical Gyro<sup>20</sup>

It can also be shown that an optical source spectral width of  $\sim 100$  kHz is required to achieve OPRGs used for aircraft ( $\Omega_{SN} \sim 10^{-7}$  rad/s).

Studies are being conducted in various research institutes using experimental systems. 21-25 Figure 7 shows a system recently tested by the author, et al.

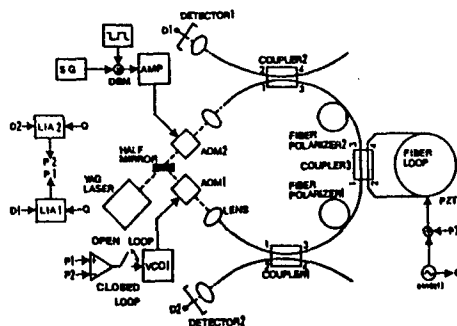


Figure 7. Passive Ring Resonance Optical Gyro Experimental System Structure<sup>22</sup>  
(Backward scattering induction noise was reduced.)

This system is used to verify a new system to reduce noise arising from the coherent component of backward scattering light and signal light.<sup>22</sup> The reduction of such noise requires that one incident light carrier component be fully suppressed<sup>21</sup> (Table 1). This system uses a modulation process called "binary phase shift keying," and provides light waves with repeated phase modulation of the order of  $0, \pi, 0, \pi$ . In this case, the carrier components are substantially removed. Such modulation is simply achieved by DBM and AOM, as illustrated, thus offering unadjusted technique.<sup>22</sup>

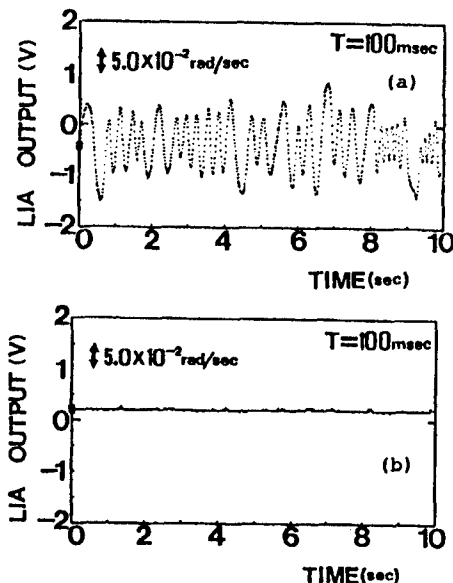


Figure 8. Results of Backward Scattering Induced Noise Reduction<sup>22</sup>  
(a) Without b-psk modulation (b) With b-psk modulation

An LD excited small-size YAG laser (output 2.5 mW, wavelength 1.32  $\mu\text{m}$ ) of about 300 kHz in spectral width (including jitter) was used for the test system. A resonator of about 40 in fineness was constructed using a polarized wave maintaining optical fiber directional coupler and polarized wave maintaining optical fibers 14 m in length. The diameter of such resonator is 10 cm. Figure 8(a) and (b) shows a comparison of noise reduction state using the above process.<sup>22</sup> Figure 9(a) [not reproduced] shows drifts<sup>22</sup> achieved as a result of such comparison. The drifts fell within a fluctuation of about  $10^{-4}\text{rad/s}$  (integral time: 10 seconds) extending over 14 minutes. The rotating detection functions were also confined, and the results are shown in Figure 9(b) [not reproduced].<sup>22</sup>

## 5. Conclusion

A trend of research and development of coherent optical fiber gyros and passive ring resonance optical gyros was outlined. All items of knowledge necessary to develop highly efficient coherent optical fiber gyros can be said to have been obtained; such gyros are in the final phase for practical use. Passive ring resonance optical gyros are still in basic research. Many studies, however, have to date been accumulated to grasp the noise factor behaviors. Passive ring resonance optical gyros are receiving much attention as ultimate sensors using coherent optical sources.

## References

1. Hotate, Higashiguchi, and Niwa, MEASUREMENT AND CONTROL, Vol 20 No 10, October 1981, pp 937-946.
2. Hotate, K., NIKKEI MECHANICAL, Vol 6 No 3, 1985, pp 75-87.
3. Ogoshi, Hishihara, Okamoto, Otsu, and Hotate, "Optical Fiber Sensor," Ohm Co., 1984, pp 205-252.
4. Hotate, K., Applied Physics Optical Fiber Sensor Study Meeting, WOFS4-15, No 1, 1987, pp 105-112.
5. Hotate, K., Laser Academic Society Research Meeting, RMT-88-32, February 1989, pp 1-6.
6. Hotate, K., ELECTRONIC INFORMATION COMMUNICATION SOCIETY JOURNAL, 1989.
7. Bergh, R.A., Refevre, H.C., and Shaw, H.J., IEEE JOURNAL LIGHTWAVE TECHNOLOGY, Vol LT-2 No 2, April 1984, pp 91-107.
8. Kim, B.Y. and Shaw, H.J., IEEE SPECTRUM, March 1986, pp 54-60.
9. Ibid., "Fiber Optic Gyros 10th Anniversary Conference," PROCEEDINGS SPIE, Vol 719, 24-26 September 1986.

10. Ibid., "Special Symposium: Optical Fiber Gyro," Applied Physics Optical Fiber Sensor Study Meeting, WOFS4, January 1987.
11. Ibid., "Laser Gyro," Laser Academic Society Research Meeting Report, 14 February 1989.
12. Hotate, K. and Tabe, K., APPL. OPT., Vol 25 No 7, April 1986, pp 1086-1092.
13. Ibid., IEEE JOURNAL LIGHTWAVE TECHNOLOGY, Vol LT-5 No 7, July 1987, pp 997-1001.
14. Moeller, R.P., Burns, W.K., Frigo, N.J., IEEE JOURNAL LIGHTWAVE TECHNOLOGY, Vol LT-7 No 2, February 1989, pp 262-269.
15. Giallorenzi, T.G., 100C'89, 20D3-1.
16. Hotate, K., Samukawa, S., and Niwa, W., Int. Conf. Optical Fiber Sensors, New Orleans, 27-29 January 1988, pp 397-400.
17. Pavlath, A., National Technical Meeting, the Institute Navigation, 26-29 January 1988, pp 91-98.
18. Laskoskie, C., Hung, H., El-Wailly, T., and Chang, C.L., IEEE LIGHTWAVE TECHNOLOGY, Vol LT-7 No 4, April 1989, pp 600-606.
19. Hotate, K., Sino-Japanese Symposium on Optical Fiber Sensors, Beijing, 8-9 November 1988, pp 39-41.
20. Iwatsuki, K., Hotate, K., and Higashiguchi, M., APPL. OPT., Vol 25 No 15, August 1986, pp 2606-2612.
21. Zarinetzi, F. and Ezekiel, S., OPT. LETT., Vol 11 No 6, June 1986, pp 401-403.
22. Hotate, K., Takiguchi, K., and Hirose, A., Inter. Conf. Integrated Optics and Opt. Fiber Commun., 100C'89, Kobe, 18-21 July 1989, pp 2D3-2.
23. Mayer, R.E., Ezekiel, S., Stowe, D.W., and Tekippe, V.J., OPTICS LETT., Vol 8 No 12, December 1983, pp 644-646.
24. Sanders, G.A., Demma, N., Rouse, G.F., and Smith, R.B., Int. Conf. Opti. Fiber Sensors, New Orleans, 27-29 January 1988, pp 409-412.
25. Takahashi, M., Tai, S., Kyuma, K., and Hamanaka, K., OPTICS LETT., Vol 13 No 5, May 1988, pp 413-415.

## Sawtooth Wave Generation Circuit on Closed Loop Fiber Gyro

906C3832H Tokyo HIKOKI SHINPOJIUMU in Japanese 18-20 Oct 89 pp 92-95

[Article by Akihiro Kurokawa, Kenichi Kajiwara, Naoki Usui, and Yoshiaki Yayakawa, Mitsubishi Precision Co., Ltd., and Masamitsu Haruna and Hiroshi Nishihara, Electronic Engineering Faculty, Osaka University]

### [Text] 1. Introduction

Fiber optical gyros (FOG) are being actively developed as the next-generation gyros. Closed loop FOGs that feed back sawtooth wave phase modulation signals, possess a wide dynamic range. They also have a possibility of obtaining superior scale factor stability and linearity. Studies, therefore, are being actively conducted concerning closed loop FOGs.<sup>1-3</sup> Of these studies, reference 1 describes theoretical studies on the effect of sawtooth wave phase modulation signal characteristics on gyro performance. References 2 and 3 also describe the results of performance tests on the entire gyro. No test data, however, have been given in these references concerning the effect of sawtooth waves on flashback time and the effect of sawtooth wave amplitude on scale factor linearity.

Experiments using closed FOGs employing light guide modulator (IOM) and sawtooth generating circuits were conducted concerning:

- 1) Effect of sawtooth wave amplitude and flyback time on scale factor linearity.
- 2) Effect of sawtooth wave amplitude fluctuation on scale factor linearity.

This paper describes the results of the above experiments.

### 2. Closed Loop FOG Demodulator Output

Figure 1 shows the structure of a closed loop FOG using an IOM and a sawtooth wave generating circuit. In this closed loop FOG, sawtooth wave phase modulation signals are applied to light propagating in the fiber loop in the reciprocating direction, in addition to sine wave phase modulating signals.



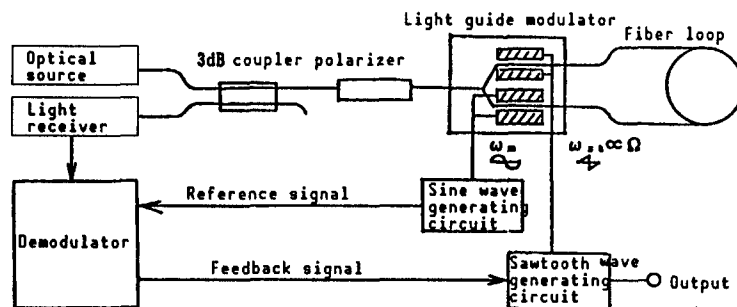


Figure 1. Closed Loop FOG Structure

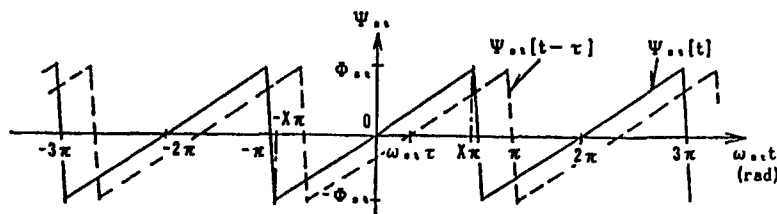


Figure 2. Sawtooth Wave Phase Modulation Function:  $\Psi_{st}$

Generally, sawtooth wave phase modulation signals possess limited flyback time, and are represented by a function  $\Psi_{st}$  shown in Figure 2,

where  $\Phi_{st}$  = maximum phase deviation of sawtooth wave phase modulation

$$X = 1 - t_f \cdot f_{st}$$

$t_f$  = flyback time

$f_{st}$  = sawtooth wave phase modulation frequency

$$\omega_{st} = 2\pi f_{st}$$

$\tau$  = fiber loop propagating delay time

$t$  = time

The demodulator picks out scalar products obtained by multiplying the strength of interference light incident on the light receiver by sine wave phase modulation signals. So far, the demodulator output signal terms, to which sawtooth wave phase modulation signals are related, have been indicated by using complex Fourier factors.<sup>1</sup> In this paper, the demodulator output signals are indicated as follows, using actual Fourier factors to facilitate the calculation of  $f_{st}$  that changes demodulator output signals to zero.

$$V = 4G \sqrt{P_{cw}P_{ccw}} \cdot J_1(\eta) \cdot \left\{ A_0/2 + \sum_{k=1}^{\infty} [A_k \cdot \cos(K\omega_{st}t) + B_k \cdot \sin(k\omega_{st}t)] \right\} \quad (1)$$

where  $G$  = factor of proportionality

$P_{cw}$  and  $P_{ccw}$  [as published] = strength of clockwise and counterclockwise light, respectively

$J_1$  = primary Bessel function

$\eta$  = phase modulation factor

$A_0$ ,  $A_k$ , and  $B_k$  = actual Fourier factor

If AC components are removed by the low bus filter, demodulator signals shown by equation (1) can be represented by the following equation:

$$V = 2G\sqrt{P_{cw}P_{cw}} \cdot J_1(\eta) \cdot A_o \quad (2)$$

where

$$\begin{aligned} A_o = & \frac{4(1-X)X}{\Phi_{st}} \cdot \sin\left(\frac{\Phi_{st}}{X}\right) \sin\left\{\phi_s - \frac{\Phi_{st}}{X} + \frac{\Phi_{st}}{X\pi} \cdot \omega_{st}\tau\right\} \\ & + \frac{1}{\pi} (2X\pi - \omega_{st}\tau) \cdot \sin\left\{\phi_s + \frac{\Phi_{st}}{X\pi} \cdot \omega_{st}\tau\right\} \\ & + \frac{1}{\pi} \{2(X-1)\pi + \omega_{st}\tau\} \cdot \sin\left\{\phi_s - \frac{\Phi_{st}}{X\pi} (2\pi - \omega_{st}\tau)\right\} \end{aligned} \quad (3)$$

$\phi_s$  = Sagnac phase difference

A closed loop FOG has a feedback loop that changes sawtooth wave phase modulation frequency  $f_{st}$  so that the demodulator output signals amount to zero. In this case, where  $t_f = 0$  (that is,  $X = 1$ ),  $\Phi_{st} = q\pi$  ( $q = \pm 1$ ), the following ideal output can be obtained:

$$f_{st} + -\frac{\phi_s}{2\pi q\tau} = -\frac{1}{q} \cdot \frac{2R}{\lambda n_f} \cdot \Omega \quad (4)$$

where  $R$  = fiber loop radius  
 $\lambda$  = wavelength in vacuum  
 $n_f$  = fiber refractive index  
 $\Omega$  = input angle speed,  $\sin(\Omega/q) < 0$

The actual sawtooth wave, however, is  $t_f \neq 0$  (that is,  $x \neq 1$ ). Since  $\Phi_{st}$  also changes, ideal outputs cannot be obtained.

Described below are the results of experiments on the effects of flyback time and sawtooth wave amplitude  $\Phi_{st}$  on scale factor and linearity.

### 3. Experiments

#### 3.1 Outline of Prototype

The closed loop FOG optical system manufactured on an experimental basis consists of a super radiant diode, grinding type 3 dB coupler, fiber polarizer, light guide modulator (IOM), polarization surface storage fiber loop, and avalanche photodiode. Regarding IOM, a Y branch light guide and two phase modulators are integrated on an X-cut Y propagation  $\text{LiNbO}_3$  substrate, in which Ti is diffused. The light guide width is  $5 \mu\text{m}$  and the branch angle of the Y branch light guide is  $1/50$  rad. Specifications of the closed loop FOG and IOM manufactured for experiments are given in Tables 1 and 2. The appearance of the closed loop FOG is also shown in Figure 3 [not reproduced].

Table 1. Specifications of Closed Loop FOG

Shape, dimensions (mm)	$\phi 110 \times 30$ (h)
Wavelength (nm)	816
Fiber - type	PANDA
- length (m)	601.3
Since wave phase modulation frequency (kHz)	170
Optical scale factor (deg/(°/sec))	0.833

Table 2. Specifications of Light Guide Modulator

Shape/dimensions of LiNbO <sub>3</sub> substrate (mm)	5(w) x 49(l) x 1 (h)
Length of electrode (mm)	27
Excess loss - light guide (dB)	2.5
- between light guide and fiber (dB)	1.3
Branch ratio (%)	44:56
Crosstalk (dB)	$\leq -17$
Half wavelength voltage (V)	4.2
3 dB bandwidth (MHz)	$\geq 800$

Further, in order to investigate effects on the gyro performance, two types (flyback time: 40 ns and 520 ns, respectively) of sawtooth wave generating circuits were manufactured for experiments. The amplitude of these circuits is changeable, and the specifications of the circuits are given in Table 3.

Table 3. Specifications of Sawtooth Wave Generating Circuit

Parameter	(A)	(B)
Frequency - range (Hz)	0.1 mHz~200 kHz	0.1 mHz~200 kHz
- probability (ppm)	$\pm 5$	$\pm 5$
- jitter (ns)	$\pm 4.4$	$\pm 75$
Flyback time (ns)	40	520
Amplitude - range at 50 $\Omega$ (V <sub>p-p</sub> )	0~10	0~15
- probability (%)	$\pm 0.2$	$\pm 0.05$
- frequency factor (%/kHz)	-0.0046	-0.037

### 3.2 Methods and Results of Experiments

#### (1) Scale Factor and Linearity

To investigate changes in scale factor and linearity arising from changes in amplitude  $\Phi_{st}$ , scale factors and linearities were measured by changing the amplitude of sawtooth waves in regard to a closed loop FOG that uses a sawtooth wave generating circuit (A) [ $t_f = 40$  ns]. Selected amplitudes  $|\Phi_{st}|$  are  $0.8\pi$ ,  $0.9\pi$ ,  $\pi$ ,  $1.1\pi$ , and  $1.2\pi$ . Next, to investigate changes in scale factor and linearity arising from differences in flyback time, similar experiments were conducted for a closed loop FOG that uses a circuit (B) [ $t_f = 520$  ns]. Experiments were conducted at an ambient temperature of  $23^\circ\text{C} \pm 2^\circ\text{C}$  without controlling FOG temperatures. Output frequency  $f_{st}$  was measured at a step of  $10^\circ/\text{s}$  from  $-100^\circ/\text{s}$  to  $+100^\circ/\text{s}$  under each amplitude. A regression line of such output frequency  $f_{st}$  was then obtained by using the method of least squares, and the scale factor was established to be the inclination of such regression line. Further, linearity was established to be the maximum value of deviations from the regression line and was indicated by a ratio to full scale.

The results of experiments on scale factor and linearity with respect to sawtooth wave amplitudes are shown in Figures 4 and 5, respectively, together with calculated values. Output frequency  $f_{st}$  that results in equation (3) becoming zero was calculated for input angle speeds extending from  $-100^\circ/\text{s}$  to  $+100^\circ/\text{s}$ , using data given in Tables 2 and 3. Thus, calculated values were obtained. Actually measured values agree well with calculated values for both scale factor and linearity.

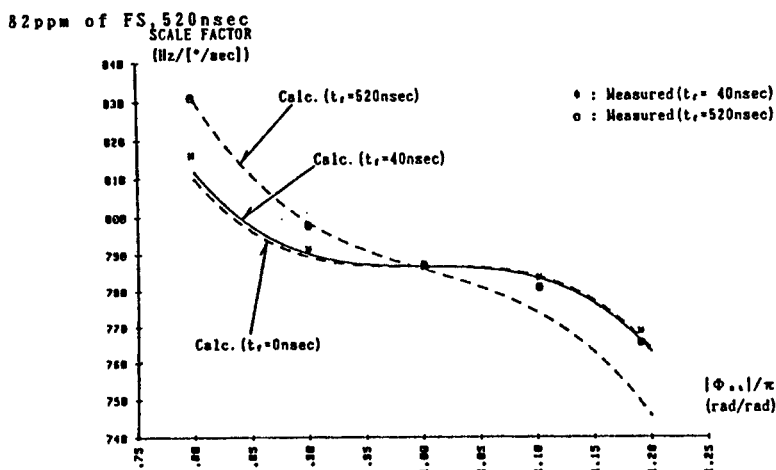


Figure 4. Relationship Between Sawtooth Wave Amplitude and Scale Factor

Figure 4 reveals the following:

- 1) A minimum scale factor fluctuation rate with respect to amplitude is  $|\Phi_{st}| = \pi$
- 2) The shorter the flyback time, the smaller the scale factor fluctuation rate.

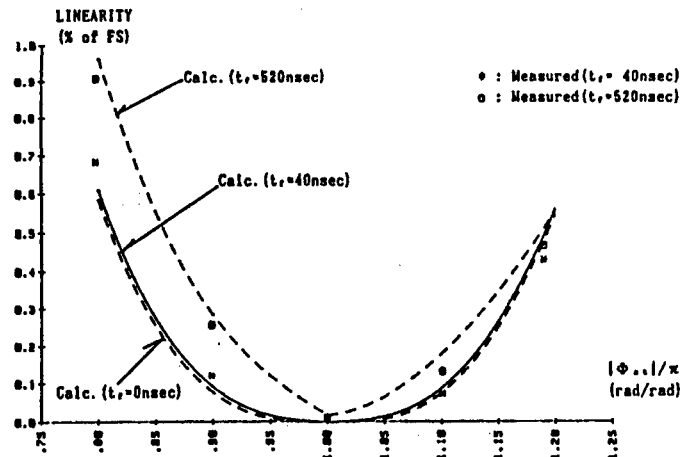


Figure 5. Relationship Between Sawtooth Wave Amplitude and Linearity

Figure 5 reveals the following:

- 1) Where  $|\Phi_{st}| = \pi$ , the most satisfactory linearity can be obtained.
- 2) The shorter the flyback time, the better the linearity.

Where  $|\Phi_{st}| = \pi$ , the following linearities were obtained. FS was  $100^\circ/\text{s}$   
 82 ppm of FS at a flyback time of 40 ns  
 132 ppm of FS at a flyback tie of 520 ns

## (2) Scale Factor Stability

To confirm the experimentally manufactured closed loop FOG scale factor stability, the sawtooth wave amplitude (nominal):  $\Phi_{st}$  was established to be  $|\Phi_{st}| = \pi$ . The scale factor stability of the prototype was then measured using circuits (A) and (B). One or more hours were taken as cool-down time between each measurement. Scale factor measurements as in the case of (1) above were carried out five times, and a standard deviation of five scale factors was obtained. Thus, the scale factor stability was represented by the ratio to the average of scale factors.

Actual measured scale factor stabilities were as follows:

Where circuit (A) was used, 13.8 ppm (1  $\sigma$ ).  
 Where circuit (B) was used, 38.2 ppm (1  $\sigma$ ).

Meanwhile, scale factor stabilities calculated using equation (3) and Tables 2 and 3 data were as follows on the assumption that the sawtooth wave amplitude stability is determined based on circuit output amplitude stability.

Where circuit (A) (flyback time: 520 ns, amplitude fluctuation:  $\pm 0.2\%$ ) is used, 11.7 ppm (1  $\sigma$ ).  
 Where circuit (B) (flyback time: 520 ns, amplitude fluctuation:  $\pm 0.05\%$ ) is used, 40.3 pm (1  $\sigma$ ). In this case, the circuit amplitude was assumed to fluctuate at random and also to be a normal distribution.

Calculated values agree well with actual measured values. This has made it clear that scale factor stability is subject to the fluctuation of sawtooth wave generating circuit amplitude.

#### 4. Conclusion

The relationship between circuit output characteristics and scale factors, and linearity and scale factory stability were revealed through experiments with closed loop FOGs that use light guide modulators and sawtooth wave generating circuits. Actual measured values have been confirmed to agree well with calculated values.

Generally, inertial grade gyros require a scale factor error of 100 ppm or less. Experiments conducted show that driving FOGs at an amplitude of  $\pi$  for a sawtooth wave generating circuit flyback time of 40 ns or less results in highly accurate FOGs. The bias stability of closed loop FOGs used for the experiments was 0.43°/hr (1  $\sigma$ ).

#### References

1. Ebberg, A. and Schiffner, G., OPTICS LETTERS, Vol 10 No 6, 1985, p 300.
2. Lefevre, H.C., "Fiber Optic and Laser Sensors V," Proc of SPIE, Vol 838, 1987, p 86.
3. Pavlath, G.A., Proc. of National Technical Meeting, 1988, p 90.

## In-Flight Imaging System

906C3832I Tokyo HIKOKI SHINPOJIUMU in Japanese 18-20 Oct 89 pp 96-99

[Article by Takashi Kijima and Hiroshi Asano, Mitsubishi Electric Corp.]

### [Text] 1. Introduction

Infrared imaging systems, coupled with a small number of detecting devices, have so far obtained two-dimensional images with mechanically scanning mirrors, etc., because of problems with light receiving devices. The use of infrared imaging systems, therefore, has to date been limited to military purposes in view of equipment reliability, size, price, resolution of images, etc.

Mitsubishi Electric Corp. first developed two-dimensional devices (used for infrared rays) having the same resolution as that of a charge-coupled device (CCD) for video cameras that use visible rays. Since April 1988, these devices have been on the market as thermal imagers and have been highly evaluated by various fields. Further, the company put improved types (that can be carried by aircraft) on the market in 1989. This paper briefly describes infrared rays, features of the product, etc.

### 2. Characteristics of Infrared Rays

All objects radiate electromagnetic waves (to the outside) having strength determined by temperature and emissivity. If the emissivity remains constant, all radiant energy of the object is proportional to the fourth power of the object temperature. In the case of objects whose temperature is maintained at approximately room temperature, the wavelength of radiant energy at its peak falls within the far infrared ray region of about 10  $\mu\text{m}$  (Figure 1).

Further, the characteristics of infrared rays propagating in the atmosphere show complicated shapes, as shown in Figure 2, because infrared rays are absorbed by various gas molecules existing in the atmosphere. Two regions of atmospheric windows have comparatively satisfactory propagating characteristics, the 8-13  $\mu\text{m}$  region and the 3-5  $\mu\text{m}$  region (medium infrared ray).

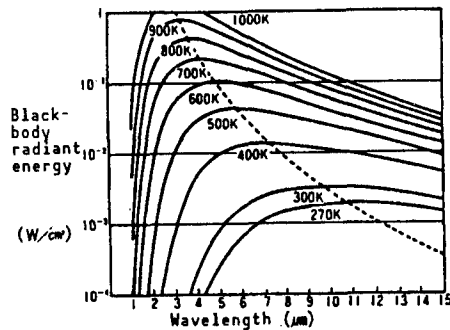


Figure 1. Blackbody Radiant Energy

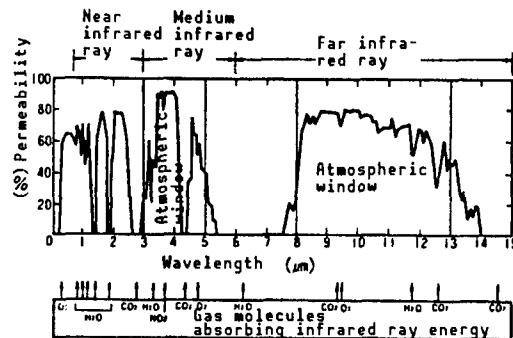


Figure 2. Spectral Permeability in Atmosphere

### 3. Imaging System

Conversion of energy radiated by objects makes it possible to image scenes in the darkness without illumination. The development and practical use of such a system, particularly for military purposes, has been carried out in many countries for 20 years.

The above system uses a wavelength in the 8-13  $\mu\text{m}$  region. As infrared ray detecting devices having the highest sensitivity, HgCdTe is used for far infrared rays and InSb for medium infrared rays. These devices, however, have difficulties in satisfying high quality and uniformity requirements. Two-dimensional images, therefore, have so far been formed by using several detecting devices and scanning mirrors that change the viewing direction of the devices. This is the major reason for the use of the 8-13  $\mu\text{m}$  wavelength region. Figure 3 shows an example, the U.S. Army's system called "common module," that scans one-dimensional linear arrays with mirrors in the horizontal direction. In this system, the detecting device looks at a direction in a moment. To achieve high sensitivity, infrared ray detecting devices have to date been developed and improved with emphasis on the 8-13  $\mu\text{m}$  region where infrared ray energy is larger by almost one order of magnitude.

Emphasis is being put on development of highly sensitive, highly resolvable, small-size, and highly reliable infrared imaging systems. The ultimate purpose for this technological development is to be able to use two-dimensional devices to eliminate the need for mechanical scanning. Figure 4 shows a sensor part using a two-dimensional device.



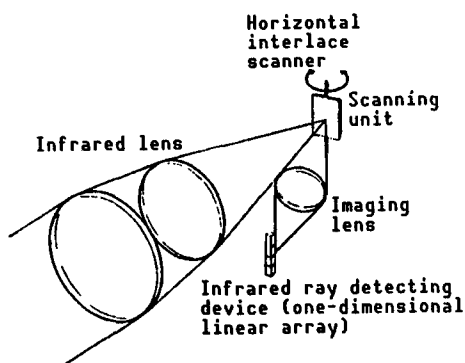


Figure 3. Scanning Mirror Infrared Imaging System

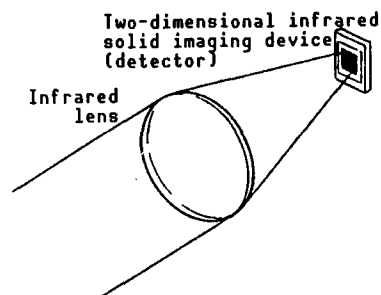


Figure 4. Two-Dimensional Infrared Imaging System

It is difficult to manufacture highly uniform, multi-devices with HgCdTe (device material), which is used for the 8-13  $\mu\text{m}$  region. In many countries, research is being conducted to develop two-dimensional devices of several thousands to 10,000 picture elements. The development of multi-devices having a higher grade is deemed to be difficult in view of the structure.

Meanwhile, it has not yet been possible to develop highly sensitive equipment for the 3-5  $\mu\text{m}$  region. Our developed two-dimensional devices with 250,000 picture elements, however, are changing the whole situation. Infrared energy emitted by objects is incommensurably small. It has become possible, however, to achieve sensitivity equivalent to that of conventional 8-13  $\mu\text{m}$  region imaging systems by accumulating 1/60 second incident energy, which corresponds to 1 field of TV display.

#### 4. IRCSD With 250,000 Picture Elements

This device is called an infrared charge sweep device (IRCSD) and uses PtSi photodiodes. Research was started by our company about 9 years ago. Development of infrared charge-coupled devices (IRCCDs) made of PtSi was proposed by Shepherd, et al., of the U.S. Air Force Research Laboratory in 1973. In those days, not many manufacturers tackled development of such a device. IRCCDs, however, are now being developed by many firms, stimulated by recent progress in the technology. Figure 5 shows a simple device (4 x 4 in picture element) to explain structure and operation peculiar to our developed IRCSDs.

With respect to conventional CCDs, it is difficult to provide the light detectors with a large space in the device, and, therefore, the sensitivity lowers. Our CSDs were developed by improving this defect.

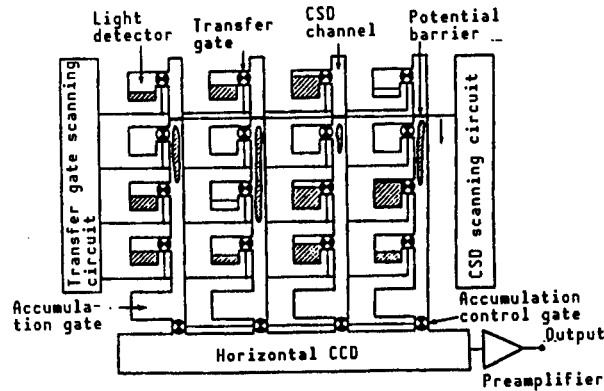


Figure 5. Structure and Operation of CSD Device

Described below are the features of an infrared imaging system using IRCSD.

- 1) The system shows its sensitivity to infrared rays in the  $3\text{--}5\ \mu\text{m}$  in wavelength region.
- 2) The system is a two-dimensional staring sensor.
- 3) The number of picture elements is  $512 \times 512$ , which show an extremely high resolution as an infrared system.
- 4) The base material is pure Si (silicon).

A comparison of the  $3\text{--}5\ \mu\text{m}$  region with  $8\text{--}13\ \mu\text{m}$  region is summarized below.

- (1) The amount of infrared rays (emitted by objects) of  $8\text{--}13\ \mu\text{m}$  wavelength is larger by one figure or more than that of infrared rays of  $3\text{--}5\ \mu\text{m}$  wavelength.
- (2) The atmospheric permeability of infrared rays of  $3\text{--}5\ \mu\text{m}$  wavelength under comparatively good visibility does not fluctuate according to seasons. Infrared rays of  $8\text{--}13\ \mu\text{m}$  wavelength, however, are greatly absorbed and attenuated by steam, and the atmosphere permeability greatly fluctuates according to seasons. This state is shown by the results of calculations (Figure 6).

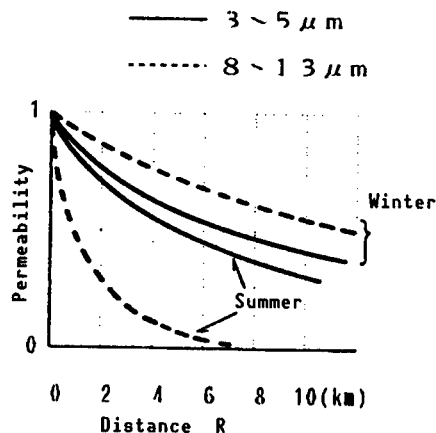


Figure 6. Comparison of Atmospheric Permeability

(3) The permeability of infrared rays in haze, mist, etc. is satisfactory when compared with visible rays, because of the long wavelength. Further, infrared rays of 8~13  $\mu\text{m}$  wavelength are slightly superior in permeability to those of 3~5  $\mu\text{m}$  wavelength.

(4) The particle size of mist, cloud, rain, etc., is equivalent to or larger than the wavelength of infrared rays. Therefore, there are no differences in permeability arising from differences in wavelength.

Further, the use of two-dimensional staring sensors (mentioned in (2) above) has achieved a high sensitivity even in regard to infrared rays of 3~5  $\mu\text{m}$  wavelength (not emitted by objects in large quantities). The high resolution of 512 x 512 picture elements can display image information on TV screens to the maximum extent possible. The system uses Si as a base material, as in the case of general LSIs. This makes it possible to apply advanced process technologies, thereby offering high-quality devices at low cost in large quantities. The use of conventional HgCdTe results in an extremely expensive imaging system, due to an increase in the number of devices and yield, for the same resolution as that of the IRCSD infrared imaging system.

Because infrared imaging has to date been employed mainly for military purposes, it is expected that IRCSD imaging systems can widely cover fields other than military purposes. Carrying IRCSD imaging systems, particularly by aircraft, may add significant contributions to aircraft taking off and landing at nighttime and poor visibility, navigation support, rescuing, search, etc.

## 5. Latest IRCSD Imaging System

Figure 7 [not reproduced] shows an IR-5120 put on the market this year. The basic components of this system are a camera head and a camera controller. The camera head, with a standard 50-mm lens, can be hand-held. A Stirling cycle cooler, to operate the device at a temperature of about 80 K, is inside the camera head. The camera controller uses a primary power source of 28 V DC, so that it can be easily operated by aircraft, etc. An adapter is located under the camera controller to ensure that the controller can be operated at AC 100 V.

The major specifications of the infrared imaging system are described below.

- Camera head dimensions and weight: 145 x 170 x 350, 7.5 kg
- Controller dimensions and weight : 200 x 200 x 450, 13 kg
- Standard lens : f:50 mm, F:1.2
- Visual field angle : 14° x 11°
- Noise equivalent temperature difference: 0.15°C
- Field time : 1/60 second
- Cooling system : S.C. cooler
- Input power supply : DC 22~28 V
- Power consumption : 250 W or less
- Option: Various types of lenses (zoom lens, etc.), shoulder pad, view finder remote control panel, digital output, false color, etc.

## Optical Applied Equipment in Aeronautical Field

906C3832J Tokyo HIKOKI SHINPOJIUMU in Japanese 18-20 Oct 89 pp 100-103

[Article by Daigen Kuroshima and Shunichi Nishimura, NEC Corp.]

[Text] 1. Introduction

This paper describes the principles, features, examples of practical application, etc., of typical optical-applied systems for aircraft such as airplanes, helicopters, and radio-controlled airplanes. Generally, electromagnetic waves handled by optical applied systems include not only visible rays, but also ultraviolet and infrared rays. Optical applied systems, therefore, mainly handle electromagnetic waves emitted by natural optical sources, various types of light emitting sources, laser, and heat sources (Figure 1).

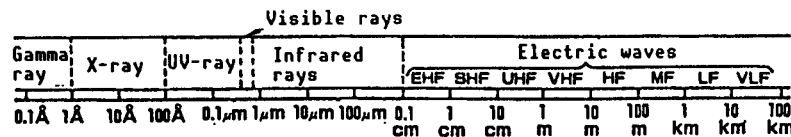


Figure 1. Electromagnetic Wave Spectrum

Table 1 presents aircraft-related optical-applied systems presently developed, including those currently under research and development.

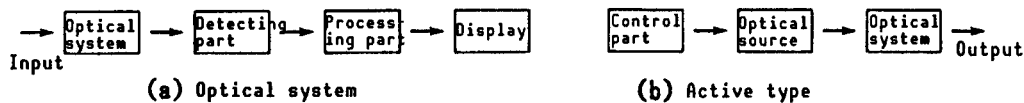


Figure 2. Basic Construction of Optical-Applied System

These optical-applied systems have a basic construction shown in Figure 2 and are characterized by the possession of an optical system.

Table 1. Optical-Applied System Related to Aircraft

<u>Navigation assisting system</u>	<u>Protective system</u>	<u>Target detecting/identifying system</u>
<ul style="list-style-type: none"> <li>• Laser gyro</li> <li>• Faint light viewing system for pilot</li> <li>• FLIR/TIS</li> <li>• Laser radar</li> <li>• Obstacle detecting system</li> </ul>	<ul style="list-style-type: none"> <li>• IRST</li> <li>• Laser security system</li> <li>• IR jammer</li> <li>• IR flare</li> </ul>	<ul style="list-style-type: none"> <li>• TV, L<sup>3</sup> TV</li> <li>• FLIR</li> <li>• IRLS, MSS</li> <li>• Laser distance measurement/irradiation unit</li> </ul>
<u>Other systems</u>	Note FLIR : Forward looking infrared TIS : Thermal imaging system L <sup>3</sup> TV : Low light level TV IRLS : Infrared line scanner MSS : Multi-spectral sensor IRST : Infrared search and track HDD : Head down display HUD : Head up display HMD : Head mounted display	
<ul style="list-style-type: none"> <li>• HDD</li> <li>• HUD</li> <li>• HMD</li> <li>• Optical data bus</li> <li>• Optical communication</li> </ul>		

## 2. Outline of Light Wave Applied Equipment

### 2.1 Faint Light Viewing System for Pilots

This system has been developed to assist the operation of helicopters during nighttime. The system is very small and lightweight, and is installed on a helmet (Figure 3 [not reproduced]). This system uses a unit called an image intensifier tube (IIT) that changes weak rays from the visible to near infrared region into electric signals, and changes again such electric signals to bright visible rays. Operation of IITs makes it possible to carry out various topographical flights at the brightness level of starlight, as in the case of daytime. (Regarding the principles of this system see Figure 4.) The visible range of this system, however, is narrow, that is, 40° (at a scale factor of 1), the same as other optical systems. Further, this system cannot distinguish thin objects such as electric wires. Due consideration, therefore, must be given to the limits of use of this system. This system can be operated for up to 40 hours by means of button-type mercury batteries and is being put into practical use for aircraft pilots.

### 2.2 FLIR/TIS

This system is an infrared imaging system or thermal image system (TIS). (FLIR (forward looking infrared) is a name used by military personnel, but is becoming a general name.) With regard to energy emitted by objects (that are merely darkness to man) at room temperature, there is a peak in infrared

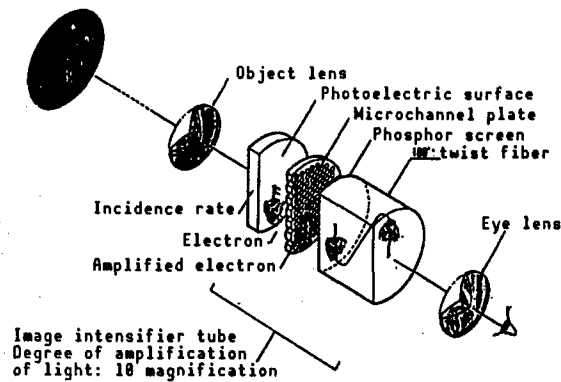


Figure 4. Principle of Faint Light Viewing System

rays of 8-14  $\mu\text{m}$ . If such energy is detected by an infrared detector, it is fully short wavelength, compared with radar, etc. Thus, it is possible to identify the shape of objects with an accuracy equivalent to that of general cameras. With the practical use of highly sensitive infrared detectors, this system is being applied to a wide range of fields because the system can image objects even in darkness where there are no visible rays. In the aeronautical field, the system is being used for navigation assisting equipment, target detecting/identifying equipment, etc. At the outset of development, single-element infrared detectors were used for the infrared imaging systems, and objects were imaged using scanners. Multielement infrared detectors, however, are being developed, and infrared imaging systems using full solid-state devices, called IRCCD, have recently been put into practical use. The infrared detector of the newly developed system, however, must be cooled to a cryogenic temperature of 80° K or less. A major feature of this system is that in good weather it can detect a man standing several km away. Further, under conditions that prevent visual observation such as fog, haze, etc., the system can detect a target by means of infrared rays. An example of this system is shown in Figure 6 [not reproduced].

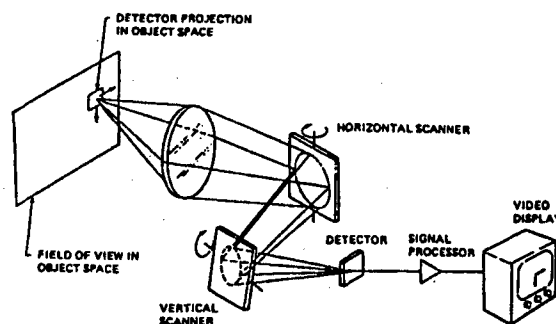


Figure 5. Principles of FLIR/TIS

### 2.3 HMD

When pilots watch the panel indicators to confirm airframe information, they move their heads upward and downward. If they wear a faint light viewing unit, the load imposed on pilots increases due to the upward and downward movement

of their heads. To reduce this load, this system was developed. Concepts of this system are shown in Figure 7. The system converts instrument information into images, and superimposes such images (in an optical manner) on the scenes viewed by the faint light viewing unit. Figure 8 [not reproduced] shows an example of practical application.

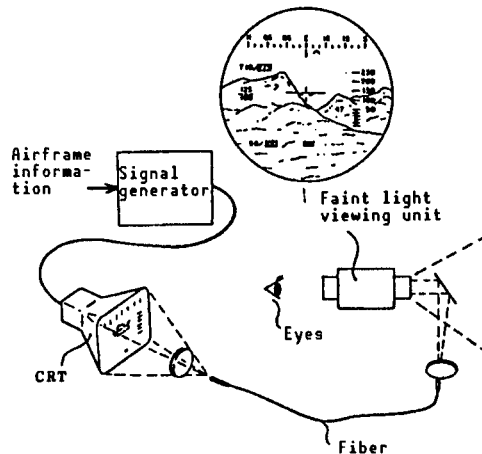


Figure 7. Concepts on HMD

#### 2.4 HUD

This system has the same functions as those of an HMD. An optical system, which changes instrument information to images and superimposes such images on outside scenes, is installed at the upper part of the instrument board. Concepts on this system and an example of practical use are shown in figures 9 and 10 [not reproduced], respectively.

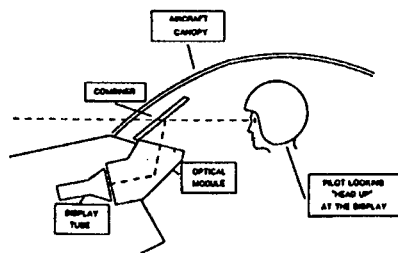


Figure 9. Concepts on HUD

#### 2.5 Obstacle Detector

This system uses CO<sub>2</sub> lasers and is being studied with a view to detecting transmission lines located 300 m away. Concepts of this system and an example of use are shown in Figures 11 and 12, respectively

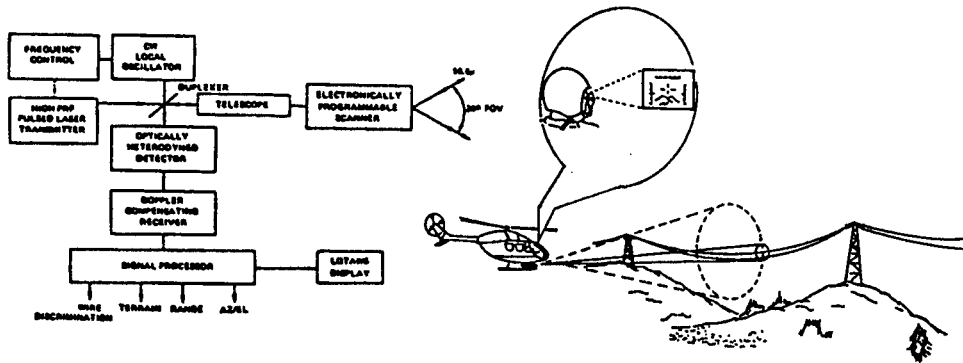


Figure 11. Concepts of Obstacle Detector

Figure 12. Obstacle Detector

### 3. Conclusion

The appearance of highly advanced and complicated aircraft requires more automated operations. Optical-applied systems, therefore, appear to have further use for the sensor and information processing fields. Many hopes are particularly placed on development of intelligent displays aimed at improving the effective utilization of display space from both software and hardware standpoints.



## STOL Aircraft HUD Radar Guidance Landing Test

906C3832K Tokyo HIKOKI SHINPOJIUMU in Japanese 18-20 Oct 89 pp 104-107

[Article by Kenji Yazawa, Kazuya Masui, and Hamaki Inoguchi, National Aerospace Laboratory; Takashi Yufuji and Shizuma Yahiro, Kawasaki Heavy Industries, Ltd.; and Hideyoshi Wakahara, (Maytech) Co., Ltd.]

### [Text] 1. Introduction

We have proceeded with development of a head-up display (HUD) as a flight test aid system for the low-noise STOL experimental plane "Asuka," and have increased its functions so that landing can be precisely carried out with radar guidance. The STOL experimental plane "Asuka" has high lifting characteristics, based on the USB system, and short-distance takeoff and landing characteristics. Flight on the back side of the V- $\gamma$  diagram, however, causes the flight-path angle response to elevators to be reversed. Small heap damping ( $Z_w$ ) also causes the response to become slow. Further, the ground effect in the vicinity of the touchdown point is large, thus involving difficulties in controlling flight. The HUD system, however, makes it possible to maintain constant pitch angles by precisely displaying attitude angles and thereby obtaining stable flight speed. The system also estimates and displays flight-path angles, thereby reducing the pilot's workload. Thus, the HUD system makes it possible to facilitate the control of planes. In particular, the precise, real-time display of flight-path angles in the vicinity of the touchdown point serves to improve the fixed-point landing performance of the STOL plane. Radar guidance provides highly accurate guidance. Data on the current position of the STOL plane, obtained by the tracking radar located at the end of the runway, are sent by telemeter to the plane concerned. Such data are passed through a complementary filter, together with inertial data to remove drift. The positional data is also smoothed, and highly accurate positional data can be obtained. A mock runway using the above data is displayed on the HUD and is overlapped with the actual runway position. This process makes it possible to easily land planes under bad weather conditions (poor visibility, etc.). Further, flight path error indications, displayed on the set flight-path, allow pilots to maintain a precise flight path, thereby improving the accuracy of fixed-point landing. NASA pilots came to Japan in 1988 and used the HUD radar guidance system to conduct evaluation tests on "Asuka." As a result,

highly accurate fixed-point landing (dispersion of three consecutive landings at the touchdown point, within 8 m) was achieved.

## 2. Outline

### • Development of HUD

Development of the HUD system for STOL experimental planes was started in 1990.<sup>1</sup> The hardware was completed in 1982, and the first simulation test was conducted<sup>2</sup> the same year. In 1983, flight tests were conducted using an experimental plane the (B-65 Queenair), and performance was evaluated. In this case, preliminary tests on radar guidance were conducted and it was confirmed that the radar guidance system is effective. In 1984, a radar guidance mode function was added to the HUD system and simulation tests were conducted. In 1985, the HUD system was carried by a STOL plane and evaluation tests were conducted. Thus, the HUD system has to date been used as a flight test aid system.

The following items were established as HUD system development targets.

- 1) In-flight mock landing tests can be carried out.
- 2) Pilots can be notified of the condition of the aircraft during flight tests.
- 3) The HUD system can be used as a landing aid during the approach of STOL and CTOL.

### • Features of HUD

In-flight mock landing is carried out to confirm the operability and landing performance of the STOL plane, as well as to gain matured experience in operation before the STOL plane actually lands on the runway. As shown in Figure 1, a mock runway is displayed on the HUD and the plane can approach the mock runway by the control method for visual flight.

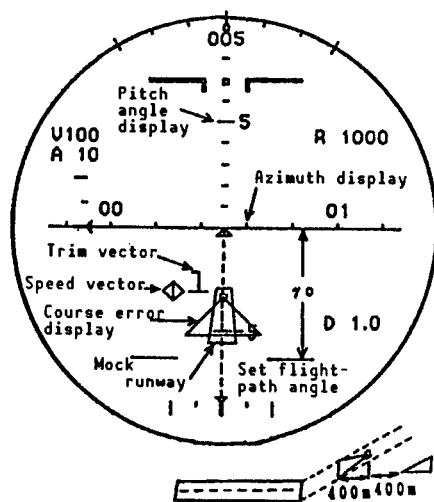


Figure 1. HUD Display Format

The HUD can integrate and display many items of information, thus making it possible to control the plane without watching other instruments. The HUD is an electronic and optical system and thereby greatly reduces delays. This makes it possible to properly control the elevating rate (flight-path angle).

HUDs can infinitely display symbols by the lens system and functions as a sort of angle indicator or angle measuring instrument, coupled with an inertial sensor offering precise attitude angles. The symbols used as angle indicators, include a speed vector indicating flight direction and a trim vector that can be used to estimate flight-path angles.<sup>3</sup> The mock runway is indicated by angles calculated based on the positional relation between the airframe and the runway.

Pitch angle indication and azimuth indication are symbols used as angle measuring instruments. These angle measuring instruments can measure angles from the aircraft at any point of the outside visual range. As a special pitch angle indication, there is a set flight-path angle indication. The set flight-path angle indication is displayed at a downward angle from the horizontal line. It is possible to judge at which of the points the aircraft is located, that is, below or above the set flight path, based on the position of the target point (that is, below or above the set flight-path angle indication). This corresponds to the glide slope error display in the instrument landing system (ILS) and microwave landing system (MLS).

### 3. Radar Guidance

Radar guidance has the following two purposes:

- 1) To precisely guide and land aircraft.
- 2) To acquire highly accurate data such as inertial sensor data.

Purpose 1) corresponds to ILS and MLS as an instrument landing aid system. The three-dimensional tracking radars used in radar guidance are equivalent in performance to MLS. Precise guidance serves to improve the fixed-point landing performance and to thereby achieve safe landing even under poor weather conditions, such as poor visual range. As one display for precise guidance, a flight-path error display is provided. In other words, a triangle (apex: 400 m away from the aircraft, base: 800 m away from the aircraft) is put on the set flight path. The pilot operates his plane toward the triangle, and the plane can automatically follow the set flight path.

The length of the triangle base is equivalent to the runway width (45 m). Thus, the pilot can guide his plane with an accuracy of about 1 m.

Speed data obtained by the inertial sensor contain a drift of about 1-3 kt, thus resulting in errors in speed vector indicating flight direction. In addition, noise occurs in radar data due to the effect of reflection of electric waves (multipath). Inertial sensor speed data drifts are removed and radar positional data are smoothed, respectively, using a complementary filter. Thus, highly accurate speed data and positional data can be obtained.

## • HUD Radar Guidance Structure

In the case of three-dimensional tracking radars, electric waves sent by the parabolic antenna are received by the transponder installed on the plane, and their frequency is slightly changed, as shown in Figure 2. Then, the electric waves are sent and received by the antenna on the ground. In this case, straight range (SR), azimuth (AZ), and elevation (EL) are measured based in time delay and direction. These data are input into a computer, converted to right-angle coordinates, and sent to the plane by the telemeter transmitter.

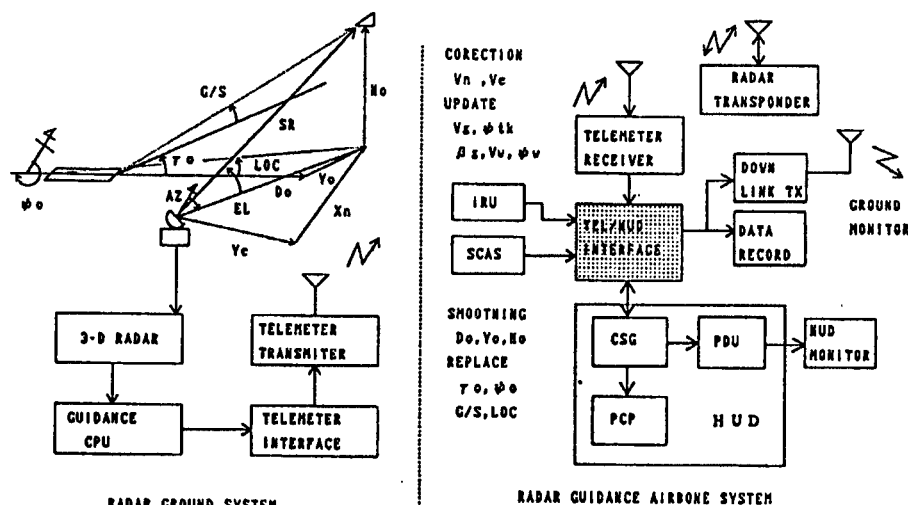


Figure 2. HUD/Radar Guidance System Structure

Data received by the telemeter receiver installed in the plane are input into the telemeter/HUD interface. Motion data sent by the inertial sensor (IUR) and air data sent by the flight control computer (SCAS), are concurrently input into the above interface. In the interface, inertial speed ( $V_n$ ,  $V_e$ ) is modified and positional data are smoothed by the complementary filter. A part of the inertial sensor data (ground speed, flying direction, sideslip angle, wind velocity, wind direction) are recalculated using modified inertial speed. Further, data output by the SCAS for in-flight mock landing are replaced with smoothed positional data ( $D_o$ ,  $Y_o$ ,  $H_o$ ) and data sent directly from the ground ( $\gamma_o$ ,  $\phi_o$ , GS, LOC). Such replacement makes it possible for the runway displayed by in-flight mock landing to agree with the actual runway.

Data modified and replaced by the interface are input into the HUD computer (CSG). When the pilot selects the radar guidance mode via the control panel (PCP), positional data ( $D_o$ ,  $Y_o$ ,  $H_o$ ) and runway direction ( $\phi_o$ ) are incorporated as initial values and a mock runway is indicated on the display (PDU).

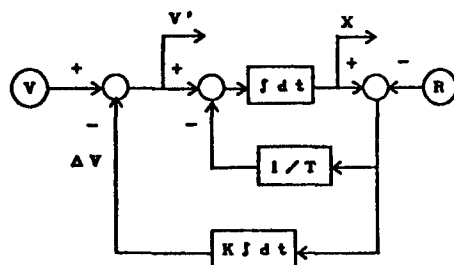
The speed of each component ( $D$ ,  $Y$ ,  $H$ ) is calculated based on ground speed ( $V_g$ ), flying azimuth ( $\phi_{tk}$ ), and course angle ( $\gamma$ ). These items of data are then integrated and positional data ( $D$ ,  $Y$ ,  $H$ ) are obtained. Where a difference of 5 m or more occurs between input and calculated positional data, initial values are renewed.

Further, where the flight path control (FPC) mode is selected, the reaching flight-path angle is estimated based on FPC lever inputs and is replaced with trim vector, which is used as reference for flight-path control.<sup>3</sup>

The radar guidance state can be monitored by the HUD monitor located at the rear seat of the experimental plane and by the real-time monitor located on the ground via the downlink.

#### • Complementary Filter

The complementary filter compensates inertial speed drifts and smoothes radar data. As shown in Figure 3, the complementary filter obtains position (X) by integrating speed (V), and compares position (X) with radar position (R). The filter then integrates speed (V) by multiplying the positional error by feedback gain (K) and feeds back such data as a speed compensation term ( $\Delta V$ ). To avoid the vibration of the filter, data are fed back by multiplying errors by a damping factor ( $1/T$ ). Thus, modified speed ( $V'$ ) and smoothed position can be obtained. Feedback gain (K) and damping factor ( $1/T$ ) were determined based on radar noise frequency components and filter convergence speed.



V	V' or X	R
V <sub>n</sub>	$\hat{V}_n$	X <sub>n</sub>
V <sub>e</sub>	$\hat{V}_e$	Y <sub>e</sub>
V <sub>g</sub> COS ( $\psi_{TK}=\psi_0$ )	$\hat{D}_0$	D <sub>0</sub>
V <sub>g</sub> SIN ( $\psi_{TK}=\psi_0$ )	$\hat{Y}_0$	Y <sub>0</sub>
H <sub>0</sub>	$\hat{H}_0$	H <sub>0</sub>

Figure 3. Complementary Filter Structure and Input/Output

#### 4. Results of Flight Tests

With respect to flight tests using the STOL experimental plane "Asuka," HUD function confirmation tests were conducted within the company. Since then, HUDs have successfully been used as flight test aid equipment. In particular, HUDs have so far been used for attitude angle control to maintain required speeds, flight balance control by trim display, approaching/landing control by flight path display, digital reading of altitude, speed, angle of attack, etc., and matured experience/evaluation by in-flight mock landing, etc.

In November 1988, evaluation tests were conducted by two pilots of NASA-Ames. Flight tests were conducted for taking off and landing performance, operability, control rules, radar guidance, etc. Flight tests were conducted 5 times during which in-flight mock landing tests were carried out 4 times and radar guide tests were carried out 17 times. One of the two pilots carried out in-flight mock landing twice. He was able to prove a high fixed-point landing performance, that is, 8 m in landing dispersion at the touchdown point, in the first three landings, as shown in Table 1. The pilot highly evaluated the following matters.

- In-flight mock landing is effective for evaluation of matured experience and flight characteristics.
- The mock runway agrees well with the actual runway in HUD radar guidance.
- Speed vectors and flight-path error displays prove to be very effective for flight path modification.

Table 1. Landing Dispersion at Touchdown Point and Flight-Path Error

Flight number	Touchdown point Do (m)	Flight-path error (m rms)	Remarks
F222-4	351.7	3.0	HUD radar
F222-5	350.7	5.6	HUD radar
F222-6	358.0	2.3	HUD radar
F223-1	-	5.6	Mock landing
F227-1	(377.8)	10.0	No HUD

## 5. Conclusion

HUDs and radar guidance systems developed as flight test aid systems for the low-noise STOL experimental plane "Asuka" have proved to be effective in properly notifying the flight condition of the plane (being tested) to the pilot and thereby helping the pilot to properly form judgments and control his plane. In addition, it has been revealed that in-flight mock landing makes it possible to safely evaluate the matured experience in the landing operation of the developed aircraft and flight characteristics of the developed aircraft at a high altitude. It has also been proved that radar guidance using HUDs is effective in ensuring the fixed point performance necessary for landing STOL planes.

We intend to mount HUDs on aircraft other than "Asuka" and to study the possibility of coupling with a general landing aid system such as MLS and the possibility of Category 3 instrument landing.

### References

1. Yazawa, et al., "Radar Guidance Using HUD," Collection of Aircraft Symposium Lectures, October 1985.
2. Tanaka, et al., "Low-Noise STOL Experimental Plane 'Asuka' Head Up Display (HUD) Primary Simulation Evaluation Tests," Aerospace Technology Research Institute data, TM-554, October 1986.
3. Masui, et al., "STOL Experimental Plane 'Asuka' Flight-Path Angle Response Delay and Display of Estimated Flight-Path Angle (in which response delay was compensated) on HUD," Collection of Aircraft Symposium Lectures, October 1989.

## Estimated Flight-Path Angle Display

906C3832L Tokyo HIKOKI SHINPOJIUMU in Japanese 18-20 Oct 89 pp 108-111

[Article by Kazuya Masui and Kenji Yazawa, National Aerospace Laboratory; Ryuji Yufuji, Kawasaki Heavy Industries, Ltd.; and Katsuhito Akashi, Shin Meiwa Industry Co., Ltd.]

### [Text] 1. Introduction

A STOL experimental aircraft "Asuka" succeeded in the first STOL landing in March 1988. Later, flight tests were conducted for 1 year to establish a STOL landing control method and to investigate an optimum landing mode. The last flight test was conducted on 30 March 1989, and thus all flight tests extending for 3 and 1/2 years were completed.

"Asuka" employs the USB system and controls flight-path angles by directly changing its lift through the operation of the engine driving force. The USB system, however, involves delays in flight-path angle response for the pilot's operation. This is one of the problems with aircraft control during STOL landing. To solve such a problem, flight path control (FPC) levers, in which delays in flight-path angle response due to engine driving force operations are compensated for by the spoiler steering, were employed; those levers improved operability. A flight-path angle response delay of about 2-4 seconds, however, was still observed. Further, since the ground effect greatly affected the flight-path angle, appropriate flare operations are required to carry out a fixed-point touchdown.

Estimated flight-path angles, in which delays in flight-path angle response are compensated by the FPC lever, were calculated and displayed on the head-up display (HUD) installed in the cockpit. Thus, loads imposed on the pilot in flight-path control during STOL landing were attempted to be reduced. This process was compared with a trim vector having flight-path angle estimating functions.

### 2. Flight-Path Angle Response Temporary Delay Approximation

The spoiler is rigged up beforehand, and the engine driving force is increased or decreased. Then, using the spoiler washout, the flight-path angle response



can be improved. This is the flight-path angle control by the FPC lever.<sup>1</sup> Figure 1 shows response to FPC lever stepped inputs. This figure shows response at a USB flap of 46° and an outboard flap of 65°; each symbol shows the following:

- $\delta_{FPC}$  = FPC lever angle
- $\gamma$  = flight-path angle
- $\delta_{SP}$  = spoiler steering angle
- $N1$  = number of engine fan rotations
- CAS = calibrated airspeed

Time and gain constants are obtained by temporary delay approximating flight-path angle response to FPC lever inputs, shown in Figure 1.

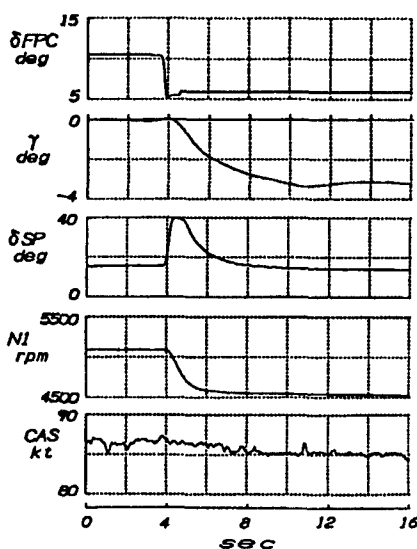


Figure 1. Flight-Path Angle Response to FPC Lever Stepped Input  
(46/65 shape)

In this case, to eliminate the effect of flight-path angle fluctuations due to changes in wind velocity, the following procedures were used.

- $C_L$  and  $C_D$  are represented by the function of elevation, thrust factor, and spoiler steering angle based on flight test data. Then, a simulation model for flight-path angle response is prepared.<sup>2</sup>
- Flight-path angles are calculated using the simulation model by inputting  $N1$ , spoiler steering angle, attitude angle, and measured wind velocity. Thus, the reproducibility of flight-path angle response measured through flight tests is confirmed.
- Flight-path angle response is calculated by simulation using measured  $N1$ , spoiler steering angle, and attitude angle with only wind velocity assumed to be constant. Thus, flight-path angle response not affected by changes in wind velocity can be obtained.

- The obtained flight-path response is approximated as a temporary delay response with respect to the FPC lever angle. Thus, time and gain constants are obtained.

The time constant and gain constant (obtained through the above procedures) of the flight-path angle response to FPC lever inputs shown in Figure 1, were 2.5 seconds and 0.85 seconds, respectively.

### 3. Structure of Delay Compensation Circuit and Display on HUD

As a result of calculations carried out in the preceding section, the flight-path angle response to FPC lever inputs is approximated by the following equation.

$$\gamma = \frac{k}{T \cdot s + 1} \delta_{FPC} \quad (1)$$

where T = time constant  
k = gain constant  
s = differentiation

To compensate for a delay of  $\gamma$ , the following equation is added to  $\gamma$ .

$$\Delta\gamma = \frac{k \cdot T \cdot s}{T \cdot s + 1} \delta_{FPC} \quad (2)$$

From equations (1) and (2),

$$\gamma + \Delta\gamma = k \cdot \delta_{FPC} \quad (3)$$

$\gamma + \Delta\gamma$  always becomes equal to the flight-path angle  $k \cdot \delta_{FPC}$  in the stationary state in equation (1).

Symbols displayed on the HUD are shown in Figure 2.<sup>3</sup> The HUD trim vector shows acceleration in the aircraft flying direction, and the reference point shows the current flight-path angle. Consequently, if  $\Delta\gamma$  signal is displayed using a trim vector symbol instead of acceleration in the flying direction, the end of the trim vector shows an estimated flight-path angle, in which flight-path angle delays are compensated. Such estimated flight-path angle is effective only during the use of the FPC lever.  $\Delta\gamma$ , therefore, is automatically changed over to the estimated flight-path angle during the use of the FPC lever. For other cases the system has been designed in such a way that accelerations in the aircraft flying direction can be displayed as usual. Further, trim vectors show acceleration, and the noise components must be removed to ensure that vectors can be easily observed. To this end, trim vectors are displayed on the HUD through a temporary delay filter of 0.2 seconds in time constant,  $T_H$ . Therefore,  $\Delta\gamma$  is also displayed through the same filter, and an estimated flight-path angle  $\gamma_{HUD}$  is displayed on the HUD using equation (4).

$$\gamma_{HUD} = \frac{1}{T_H \cdot s + 1} \Delta\gamma + \gamma \quad (4)$$

The above estimated flight-path angle  $\gamma_{HUD}$ , however, has the following two problems. First, to simplify the delay compensation circuit, the time constant and gain constant of the flight-path angle response remain fixed. This causes errors in estimated flight-path angles according to changes in flight conditions, such as flap style, speed, elevation, and thrust. Second, only changes in flight-path angles arising from FPC lever operation are considered for  $\gamma_{HUD}$ , but those in flight-path angles arising from changes in wind velocity are not considered.

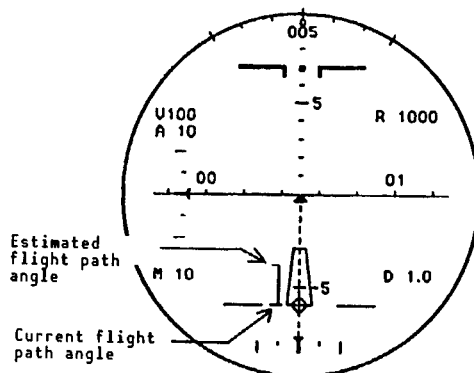


Figure 2. Display of Estimated Flight-Path Angle on HUD

#### 4. Estimation of Flight-Path Angle by Trim Vector

It is assumed that with respect to trim vectors (acceleration in the aircraft flying direction) so far displayed on HUDs, forward and backward accelerations are converted to flight-path angles during ascending and descending, respectively. This assumption makes it possible to estimate changes in flight-path angles.<sup>4</sup> This process is used to estimate flight-path angles under a balanced state by directly measuring the force applied to the aircraft. Flight-path angle response, therefore, is not likely to be affected by changes in flight conditions.

Trim vectors, however, cannot compensate delays in engine response to FPC lever operation. Further, where aircraft having backside characteristics are subjected to gusts from the forward and backward directions, trim vectors estimate flight-path angles reverse to actual flight-path angle response. In the case of a following wind, for example, forward-facing force is applied to aircraft, and trim vectors estimate increases in flight-path angle. However, since airspeed actually decreases, the aircraft descends, contrary to estimation.

#### 5. Evaluation Based on Flight Test Data

The display of estimated flight-path angles (set forth in Section 3) on the HUD is evaluated using flight test data. Flight-path angles estimated and displayed on the HUD during flight tests are not recorded as data. Such displayed flight-path angles, therefore, are quantitatively evaluated by calculating  $\gamma_{HUD}$  using equation (4).

The results of calculations on  $\gamma_{HUD}$  for FPC lever step inputs (shown in Figure 1) and measured flight-path angles are shown in Figure 3. From Figure 3, it can be seen that  $\gamma_{HUD}$  indicates steady-state flight-path angles almost concurrently with the operation of the FPC lever. Figure 4 also shows a comparison between  $\gamma_{HUD}$  and measured functions during STOL landing/approaching under the same flap style. In Figure 4,  $U_w$  shows forward/backward wind velocity (following wind: positive) and  $W_w$  shows upward/downward wind velocity (lowering wind: positive). In the first half of Figure 4,  $\gamma_{HUD}$  shows approximately the estimated changes in flight-path angle and FPC lever operation. In the latter half,  $\gamma_{HUD}$  takes a waveform, in which the phase of measured values was advanced. Thus, changes in flight-path angle are almost estimated.

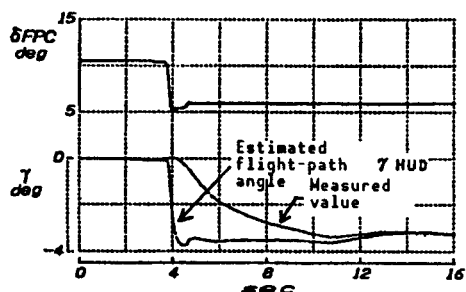


Figure 3. Estimated Flight-Path Angle on Step Input

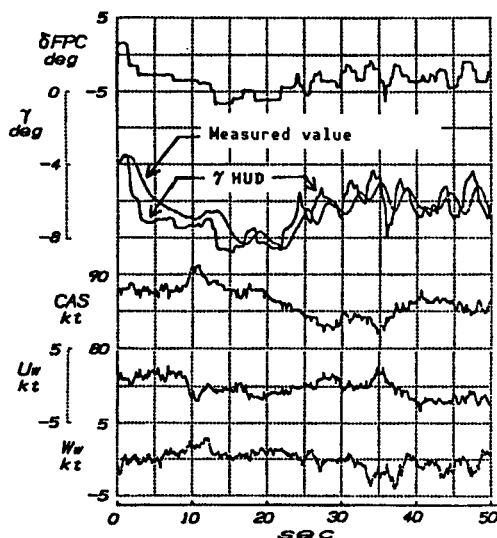


Figure 4. Estimated Flight-Path Angle During Landing/Approaching

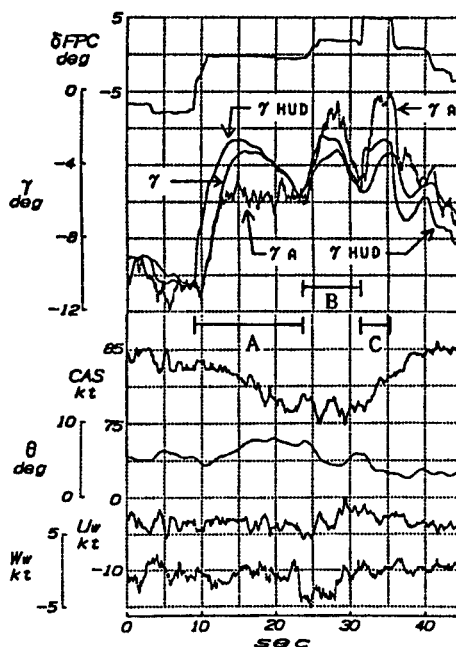


Figure 5. Comparison of Trim Vector and Estimated Flight-Path Angle

Figure 5 shows a comparison of estimated flight-path angle  $\gamma_A$  based on acceleration in the aircraft flying direction and  $\gamma_{HUD}$  and measured flight-path angle  $\gamma$  during STOL landing/approaching.

At section A in Figure 5, the attitude angle  $\theta$  has increased after operation of the FPC lever. Consequently, the flight-path angle once increased and then decreased by the amount equivalent to a decrease in CAS, resulting in a balanced state. This is because "Asuka" has backside characteristics in the adjacent flight region. In this case,  $\gamma_{HUD}$  estimates flight-path angles under a balanced state immediately after operation of the FPC lever. Later, the flight-path angle once increases, together with the actual flight-path angle, and again returns to the flight-path angle under the balanced state. Meanwhile,  $\gamma_A$  estimates a flight-path angle under the balanced state about 2 seconds after operation of the FPC lever and maintains such flight-path angle until the aircraft is placed in a balanced state.

At section B in Figure 5, the flight-path angle changes, although the FPC lever angle remains constant. This is because gusts occur in the upward/downward directions. In this case,  $\gamma_{HUD}$  does not estimate changes in flight-path angles due to gusts, but changes together with flight-path angles  $\gamma$  and does not cause large errors. Meanwhile,  $\gamma_A$  is also affected by gusts in the upward/downward directions as in the case of  $\gamma_{HUD}$ . In addition, overshooting arising from a decrease in contrary wind (following wind) can be seen.

At section C in Figure 5, CAS increases due to a decrease in attitude angle during operation of the FPC lever, unlike section A.  $\gamma_A$  shows balanced flight-path angles after a decrease in attitude angle.  $\gamma_{HUD}$ , however, does not consider changes in flight-path angle due to changes in attitude angle and shows lower values compared with  $\gamma_A$ . The reason that actual flight-path angle  $\gamma$  becomes lower than  $\gamma_A$  is because the FPC lever is pulled and the aircraft starts descending before it reaches a balanced state.

## 6. Evaluation of Flight Test

At the flight tests, the pilot commented that estimated flight-path angles can be used as reference for flight-path angle control by the FPC lever during STOL landing, in which radar guidance<sup>5</sup> is concurrently used.

In the case of STOL using a HUD as shown in Figure 6, the flight-path angle is promptly modified using the FPC lever, so that  $\gamma_{HUD}$  is maintained at  $-6^\circ$  with respect to changes in flight-path angle due to wind occurring upward and downward. The flight-path angle, therefore, is maintained approximately at  $-6^\circ$  up to an altitude of about 50 feet. Later, appropriate flare operations were carried out, and the extension of the touchdown point cannot be seen. However, where HUDs are not used, as shown in Figure 7, modification of the flight-path angle with respect to upward/downward winds can hardly be seen. The flight-path angle fluctuation range during the aircraft approach into the runway is larger compared with Figure 6. Further, from an altitude of about 100 feet, flare operations were gradually carried out, thereby causing the touchdown point to be extended, due to ground effect.

With respect to statistical evaluation concerning the maintaining of the required flight-path angle during flight tests, sufficient data were not obtainable because of the limited flight test period.

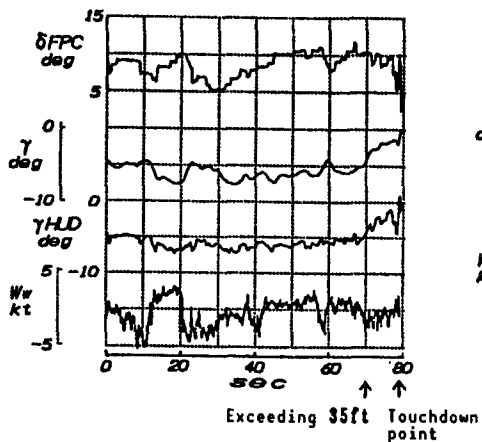


Figure 6. Landing/Approaching Using HUD

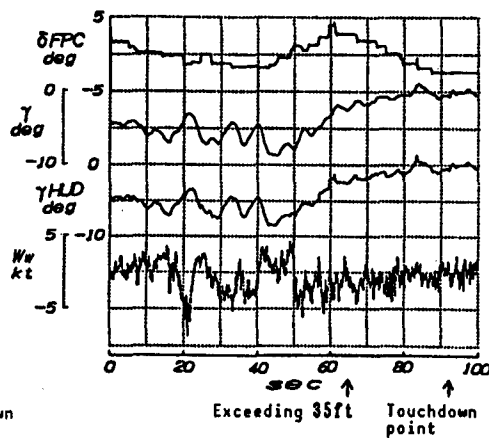


Figure 7. Landing/Approaching Without Using HUD

## 7. Conclusion

Flight tests were conducted by displaying estimated flight-path angles (in which delays in flight-path angle response for FPC lever operation were compensated) on a HUD. As a result, it has been shown that such estimated flight-path angles displayed on a HUD can be used as reference data for the control of approaching flight-path angles. It should be noted, however, that errors occur in estimated flight-path angles according to flap styles, changes in attitude angles, etc., and that no consideration is given to changes in flight-path angles that arise from changes in wind velocity. No errors due to changes in flight conditions occurred in trim vectors using acceleration in the aircraft flying direction, although errors due to changes in wind velocity in the forward/backward directions pose problems. Resolving these problems will make HUD more serviceable to flight-path angle control.

## References

1. Yamato, H., et al., "Flight Test of the Japanese USB STOL Experimental Aircraft 'Asuka,'" AIAA-88-2180, May 1988.
2. Masui, et al., "Motion Response Characteristics of Powered Lift Aircraft in the Vicinity of Ground," 26th Aircraft Symposium, October 1988.
3. Tanaka, et al., "First Simulation Evaluation Test on Low-Noise STOL Experimental Aircraft 'Asuka' HUD," data given by Aerospace Technology Research Laboratory, TM-554, October 1986.
4. Yazawa and Inagaki, "Landing Simulation for HUD," 12th Annual Meeting of Japan Aerospace Academic Society, April 1981.
5. Yazawa, et al., "HUD Radar Guidance Landing Test by STOL Experimental Aircraft, 'Asuka,'" 27th Aircraft Symposium, October 1989.

-END-

22161

17

NTIS

ATTN: PROCESS 103  
5285 PORT ROYAL RD  
SPRINGFIELD, VA

22161

This is a U.S. Government publication. Its contents in no way represent the policies, views, or attitudes of the U.S. Government. Users of this publication may cite FBIS or JPRS provided they do so in a manner clearly identifying them as the secondary source.

Foreign Broadcast Information Service (FBIS) and Joint Publications Research Service (JPRS) publications contain political, military, economic, environmental, and sociological news, commentary, and other information, as well as scientific and technical data and reports. All information has been obtained from foreign radio and television broadcasts, news agency transmissions, newspapers, books, and periodicals. Items generally are processed from the first or best available sources. It should not be inferred that they have been disseminated only in the medium, in the language, or to the area indicated. Items from foreign language sources are translated; those from English-language sources are transcribed. Except for excluding certain diacritics, FBIS renders personal and place-names in accordance with the romanization systems approved for U.S. Government publications by the U.S. Board of Geographic Names.

Headlines, editorial reports, and material enclosed in brackets [ ] are supplied by FBIS/JPRS. Processing indicators such as [Text] or [Excerpts] in the first line of each item indicate how the information was processed from the original. Unfamiliar names rendered phonetically are enclosed in parentheses. Words or names preceded by a question mark and enclosed in parentheses were not clear from the original source but have been supplied as appropriate to the context. Other unattributed parenthetical notes within the body of an item originate with the source. Times within items are as given by the source. Passages in boldface or italics are as published.

#### SUBSCRIPTION/PROCUREMENT INFORMATION

The FBIS DAILY REPORT contains current news and information and is published Monday through Friday in eight volumes: China, East Europe, Soviet Union, East Asia, Near East & South Asia, Sub-Saharan Africa, Latin America, and West Europe. Supplements to the DAILY REPORTs may also be available periodically and will be distributed to regular DAILY REPORT subscribers. JPRS publications, which include approximately 50 regional, worldwide, and topical reports, generally contain less time-sensitive information and are published periodically.

Current DAILY REPORTs and JPRS publications are listed in *Government Reports Announcements* issued semimonthly by the National Technical Information Service (NTIS), 5285 Port Royal Road, Springfield, Virginia 22161 and the *Monthly Catalog of U.S. Government Publications* issued by the Superintendent of Documents, U.S. Government Printing Office, Washington, D.C. 20402.

The public may subscribe to either hardcover or microfiche versions of the DAILY REPORTs and JPRS publications through NTIS at the above address or by calling (703) 487-4630. Subscription rates will be

provided by NTIS upon request. Subscriptions are available outside the United States from NTIS or appointed foreign dealers. New subscribers should expect a 30-day delay in receipt of the first issue.

U.S. Government offices may obtain subscriptions to the DAILY REPORTs or JPRS publications (hardcover or microfiche) at no charge through their sponsoring organizations. For additional information or assistance, call FBIS, (202) 338-6735, or write to P.O. Box 2604, Washington, D.C. 20013. Department of Defense consumers are required to submit requests through appropriate command validation channels to DIA, RTS-2C, Washington, D.C. 20301. (Telephone: (202) 373-3771, Autovon: 243-3771.)

Back issues or single copies of the DAILY REPORTs and JPRS publications are not available. Both the DAILY REPORTs and the JPRS publications are on file for public reference at the Library of Congress and at many Federal Depository Libraries. Reference copies may also be seen at many public and university libraries throughout the United States.